

論文 / 著書情報
Article / Book Information

題目(和文)	
Title(English)	Functional evaluation of DNA double-strand break repair protein XRCC4 associated with development and cancer risk
著者(和文)	ASAAnie Day De Castro
Author(English)	Anie Day De Castro ASA
出典(和文)	学位:博士(学術), 学位授与機関:東京工業大学, 報告番号:甲第12048号, 授与年月日:2021年6月30日, 学位の種別:課程博士, 審査員:松本 義久,千葉 敏,鷹尾 康一郎,塚原 剛彦,岩崎 博史
Citation(English)	Degree:Doctor (Academic), Conferring organization: Tokyo Institute of Technology, Report number:甲第12048号, Conferred date:2021/6/30, Degree Type:Course doctor, Examiner:,,,,
学位種別(和文)	博士論文
Category(English)	Doctoral Thesis
種別(和文)	要約
Type(English)	Outline

**Functional evaluation of DNA double-strand break repair protein XRCC4 associated
with development and cancer risk**

Ph.D. Thesis

Submitted by:

ASA ANIE DAY DE CASTRO

Guided by:

Assoc. Prof. Yoshihisa Matsumoto

**In Partial Fulfilment of the Requirements in the Degree of
Doctor of Philosophy**

**Tokyo Institute of Technology
School of Environment and Society
Department of Transdisciplinary Science and Engineering
Graduate Major in Nuclear Engineering**

June 2021

Dedicated to my son, Andrei Archibald Asa Alindogan

Acknowledgments

I am indebted to several people in the completion of this dissertation.

First and the most important gratitude is to my academic supervisor from master's to Ph.D., Dr. Yoshihisa Matsumoto. Thank you for believing in me and guiding me, and for helping me through all the challenges in every difficult step of my graduate school journey. Your wisdom is always my guide when I am lost and unsure in my academic life. You have been my academic father and my father in Japan. Thank you very much for everything. I always wish good health and great blessings to you and your family, and the Matsumoto Laboratory Family.

A special thank you as well to my U-ATOM mother, Haruka Watanabe, for being my mother in Japan and being my guide when I became a mother juggling graduate studies and family life. Thank you for encouraging me and helping me in many ways. I love you always.

To my friend Kaima Tsukada, thank you for always being ready to discuss about experiments and challenges in the laboratory. Your research dedication plus your kindness will give you the best future. You are my smartest friend, and I wish you win the Nobel Prize someday. I will always remember especially my friendship with you, Naoya and Akane during my graduate studies in Tokyo Tech.

To my thesis panel, Iwasaki-Sensei, Tsukahara-Sensei, Takao-Sensei and Chiba-Sensei, thank you for all the insights, guidance, and support, and all the time and effort given to my research. I am indebted to your kind insights and time given to my research.

To Matsumoto Lab., and my U-Atom professors and family especially to my U-Atom sister Aileen Brandt, to all the professors in the Nuclear Engineering, Mr. Isao Yoda at the Cobalt Irradiation Facility, the LANE administration office especially to Ms. Fujiwara, and all those I have known in the Nuclear Engineering course, for all the help, guidance, assistance, and the good memories. Thank you for the inspiration that everyone's hard work has given me.

To the loves of my life, Bino, my husband as well as my life's laughter partner and my goals partner; and Andrei, my son and my ultimate reason to strive harder. To my family in the Philippines, the Asa and De Castro Family, as well as the Alindogan Family, and to my friends who are like my extended family in Japan, I am thankful for the inspiration that you have given me. To all those who have helped me be a student mother, and to everyone who extended their help in any way for me to make Ph.D. a success, thank you very much for helping me do my best to graduate. Special thank you to Anna Camille Flores, Ethel Ranola, Rachel and Julius Lopez, Kath and Mark Ylagan, Emma and Ronel Roca, Jordan Madrid, Dominic Altura and Frederick Samonte.

I am always motivated to continue because of the love and kindness always extended to me by everyone. I will always make all of you who love me and care for me, proud of me.

Thank you, Lord for the wisdom. Glory be to God!

**Functional evaluation of DNA double-strand break repair protein XRCC4 associated
with development and cancer risk**

By: Anie Day DC. Asa

Tokyo Institute of Technology, 2020

Academic Supervisor: Assoc. Prof. Yoshihisa Matsumoto

ABSTRACT

XRCC4 is one of the most essential proteins for DNA double-strand break repair through non-homologous end joining. Several reports identified mutations in XRCC4 of patients with developmental diseases. There are also reports showing that a polymorphism in XRCC4, which changes its subcellular localization, is associated with increased cancer risk. This study aimed to explore the role of DNA repair function of XRCC4 in development and protection against cancer. I generated XRCC4 mutants mimicking these disease-associated mutants and cancer risk-associated polymorphism and analyzed their functional characteristics, i.e., radiosensitivity and DNA repair capability as well as protein expression and subcellular distribution. These mutants showed varying degrees of dysfunction, depending on the positions of mutations or the length of missing parts. These results highlighted the significance of XRCC4 in the regulation of normal development and protection against cancer through DNA repair, maintaining genomic integrity and stability.

SUMMARY

DNA double strand break (DSB) is the most detrimental damage that can happen to DNA. DNA DSBs occur at random upon genotoxic stresses which include ionizing radiation or as intermediates during a process called V(D)J recombination in the immune system. Eukaryotic cells have two major pathways to repair DNA DSBs: homologous recombination (HR) which precisely repair DNA DSBs using sister chromatid as a template, and non-homologous end-joining (NHEJ) which repairs DSBs by ligating two broken ends. NHEJ, which is predominant in mammalian cells and is active throughout the cell cycle, involves several key players such as DNA dependent protein kinase catalytic subunit (DNA-PKcs), heterodimeric Ku protein (Ku86 and Ku70), and the DNA Ligase IV (LIG4)-XRCC4-XLF complex. X-ray Complementing 4 (XRCC4) is one of the most essential proteins for DNA DSB repair through NHEJ pathway. XRCC4 was initially found as the gene which could restore normal V(D)J recombination and DNA double-strand break repair of Chinese hamster ovary-derived XR-1 cells. In NHEJ, XRCC4 has an active role of bridging damaged DNA to LIG4 for ligation of DNA ends. In studies in mice, deficiency in XRCC4 or LIG4 causes embryonic lethality and is associated with massive neuronal cell death, severe growth retardation and failure in neurogenesis. In recent studies, several human patients exhibiting developmental diseases such as microcephaly and growth defect, were found to harbor mutations in XRCC4. There are also reports showing that a polymorphism in XRCC4, which changes its subcellular localization, is associated with increased cancer risk. These XRCC4 mutations were found at or nearby different locations in the XRCC4 gene structure corresponding to different functionalities in its DNA repair capability. These disease-associated mutations have caused varied effect in DNA repair from less or unstable XRCC4 expression to total loss of DNA repair function. Unexpectedly, lymphocytes indicate normal immunological functions. This study aims to analyze the functional characteristics of XRCC4

mutations associated to development and cancer risk to delve deeper to the significance of the structure integrity of XRCC4 in the DNA repair, and in non-development and protection of diseases such as cancer. Human XRCC4 cDNA was obtained from polymerase chain reaction (PCR) of the cDNA pool of human T-cell leukemia MOLT-4 cells and integrated into p3xFLAG-CMV-10 plasmid to express XRCC4 protein with triple tandem FLAG epitope, or into pEGFP-C1 plasmid to express it as a fusion protein with green fluorescent protein (GFP). Mutations were introduced by PCR primers of different sequences depending upon the mutation. The entire XRCC4 open reading frame of the constructs was then verified to be the correct sequence by sequencing for all the constructs. These cDNAs of XRCC4 mutants were transfected to XRCC4-deficient L5178Y mouse leukemia (M10) cell line, obtained from RIKEN cell bank, and human osteosarcoma (U2OS) cell line. For M10 cells, plasmids were transfected by electroporation and visible colonies formed were expanded to obtain the stably transfected clones of the different mutated XRCC4 constructs. For U2OS cells, plasmids were transfected by lipofection. Cells were irradiated using ^{60}Co γ -ray source. The analysis of the expression level of XRCC4 was performed by Western blotting. The radiosensitivity of M10 cells are assessed in terms of the ability of the cells to proliferate by forming colonies in soft agarose 10-14 days after radiation exposure. Nuclear localization of U2OS cells was examined by observation under inverted fluorescence microscope. Repair of DNA double-strand breaks after radiation exposure was analyzed using the phosphorylation status (γ -H2AX) of serine 139 of histone H2AX as an index. Results showed that these disease-associated mutants showed varying degrees of dysfunction, depending upon the positions of its mutations, the length of deletions, or its proximity to significant positions associated to other NHEJ proteins. For disease-associated mutations, V83-S105del transfectant showed the highest radiosensitivity, which was close to control vector transfectant. D254Mfs*68 transfectant showed the second highest radiosensitivity with diminished protein expression. W43R, R161Q, R225X and

R275X transfectants, expressing the protein at equal or higher level than wild-type XRCC4 transfectant, showed slight but statistically significant increase in radiosensitivity compared to wild-type XRCC4 transfectants. When expressed in human osteosarcoma (U2OS) cells, R225X, R275X and D254Mfs*68 localized to the cytoplasm, whereas other mutants localized to the nucleus. As for A247S polymorphism associated to cancer risk, the mutation A247S has shown to be causing a significant change in subcellular localization of XRCC4 in U2OS cells which also reiterates the impact of conserved nuclear localization signal and phosphorylation sites of XRCC4 to its function. The significant increase in gamma H2Ax foci as compared to wild-type XRCC4 which increases after radiation exposure, indicates that A247S polymorphism and the change in location from A247S polymorphism causes deficiencies in DNA DSB repair through NHEJ which may lead to improper gene function leading to tumorigenesis and cancer development. These results highlighted that defects of XRCC4 in disease patients such as insufficiency in protein quantity and impaired functionality affects DNA repair, stressing the significance of XRCC4 in DNA repair, normal development, protection against cancer and in maintaining genomic integrity and stability.

TABLE OF CONTENTS

Chapter 1. Introduction	13
1.1 Theoretical Background	14
DNA	14
DNA Damage	15
Sources of DNA Damage	15
Radiation and DNA Damage	17
Radiation and Cell Survival	18
DNA Repair	19
Double-Strand Break (DSB) Repair	20
Non-Homologous End-Joining (NHEJ) Pathway	21
XRCC4	23
XRCC4 Mutations Associated to Development	25
1.2 Statement of the Problem	26
1.3 Objectives of the Study	26
1.4 Significance of the Study	27
1.5 Scope and Delimitation	28
1.6 Definition of Terms	28
Chapter 2. Materials and Methods	30
2.1 Cell Culture and Subculture	31
2.2 Freeze Stock and Thawing frozen cells	32
2.3 Mutagenesis	32
2.4 Transfection	39
2.5 Analysis of Functional Characteristics of XRCC4 Mutations	40
Protein Expression Level	40
Nuclear Localization	42
Radiosensitivity Analysis	42
Immunofluorescence	44
Chromatin Binding Assay	44
Laser Micro-irradiation	45
Computational Analysis	45

<i>Chapter 3. Analysis of the Functional Characteristics of XRCC4 Mutations Associated to Development</i>	47
3.1. Generation of Mutations in XRCC4 Associated to Development	48
3.2 Protein Expression Level	53
3.3. Nuclear Localization	56
3.4 Radiosensitivity	59
3.5 Structural Differences of XRCC4 Point Mutations Associated to Development	60
3.6 Discussion	62
<i>Chapter 4</i>	<i>(excluded)</i>
<i>Chapter 5. Conclusion</i>	67
<i>References</i>	70
<i>Appendix</i>	79
Appendix 1. Profile of Patients associated with XRCC4 Mutations	79
Appendix 2 - Sequence Check After Mutagenesis of XRCC4 Mutation Associated to Development	82
Appendix 3 - Sequence Check After Mutagenesis of XRCC4 Mutation Associated to Cancer Risk	88

Table of Figures

Figure 1. The DNA Structure and DNA composition.....	15
Figure 2. Sources of DNA Damage and Fate of DNA After Damage.....	16
Figure 3. NHEJ Pathway and Proteins Involved in the Pathway	22
Figure 4. XRCC4 Structure and Location of Important Sites in Its Structure	23
Figure 5. Overall Architecture of XRCC4-Ligase IV Complex (Sibanda et al. 2001) ...	24
Figure 6. PCMV10 Vector Map.....	33
Figure 7. pEGFP-C1 Vector.....	34
Figure 8. Location of XRCC4 mutation as compared to Wild-type XRCC4 structure ..	49
Figure 9. Expression levels of XRCC4 in M10-transfectants with wild-type and disease-associated mutants of XRCC4.	55
Figure 10. Localization of XRCC4 Mutations Associated to Development.....	56
Figure 11. Quantification of Subcellular localization of wild-type and disease-associated mutants of XRCC4 tagged with GFP.....	57
Figure 12. Localization of XRCC4 mutations Associated to Development without Endogenous XRCC4.....	58
Figure 13. Radiosensitivity of XRCC4 mutation associated to Development.....	60
Figure 14-22.....	(excluded)

Abbreviations

A	Adenine
AP	Apurinic/Apyrimidinic (sites)
APS	Ammonium Persulfate
BER	Base Excision Repair
BSA	Bovine Serum Albumin
C	Cytosine
CBS	Calf Bovine Serum
Co	Cobalt
DAPI	Diamidino-2-phenylindole dihydrochloride
DMSO	Dimethyl Sulfoxide
DNA	Deoxyribonucleic Acid
DNA-PK	DNA-dependent protein kinase
DSBs	Double Strand Breaks
EDTA	Ethylenediaminetetraacetic acid
FBS	Fetal Bovine Serum
G	Guanine
Gy	Gray
H	Hydrogen
HR	Homologous Recombination
H ₂ O ₂	Hydrogen Peroxide
IR	Ionizing Radiation
LB	Lysogeny Broth
Lig4	Ligase IV
mA	milliamperes
MeV	Mega Electron Volts
MPD	Microcephalic Primordial Dwarfism
MMR	Mismatch Repair
NER	Nucleotide Excision Repair
NLS	Nuclear Localization Signal
PAGE	Polyacrylamide Gel Electrophoresis

PBS	Phosphate Buffered Saline
PCR	Polymerase Chain Reaction
RAG	Recombination Activating Genes
ROS	Reactive Oxygen Species
RPA	Replication-fork Protein A
SSB	Single-Strand Break
T	Thymine
TEMED	Tetramethylethyene Diamine
T-PBS	Tween 20-containing PBS
UTR	Untranslated region
UV	Ultraviolet
XRCC4	X-ray Cross Complementing Protein 4
WT	Wild-type

Chapter 1. Introduction

Chapter 1

Introduction

1.1 Theoretical Background

DNA

The deoxyribonucleic acid (DNA) is a self-replicating carrier of hereditary material and informational component found inside living organisms. As shown in Figure 1, the DNA composition is made up of four chemical bases: adenine (A), guanine (G), cytosine (C), and thymine (T). The order, or sequence, of these bases determines the information for maintaining an organism. DNA is also composed of sugar molecule and a phosphate molecule, which together are called a nucleotide. Nucleotides are arranged in two long strands that form a spiral double-stranded helix like resembling a twisted ladder. The DNA needs to maintain a high degree of fidelity to replicate itself. In the cell cycle, the DNA must be replicated when cells are ready to divide and must be read to produce molecules necessary to carry out functions in the cell. In human cells, around 6 billion of DNA are distributed across 46 human chromosomes.

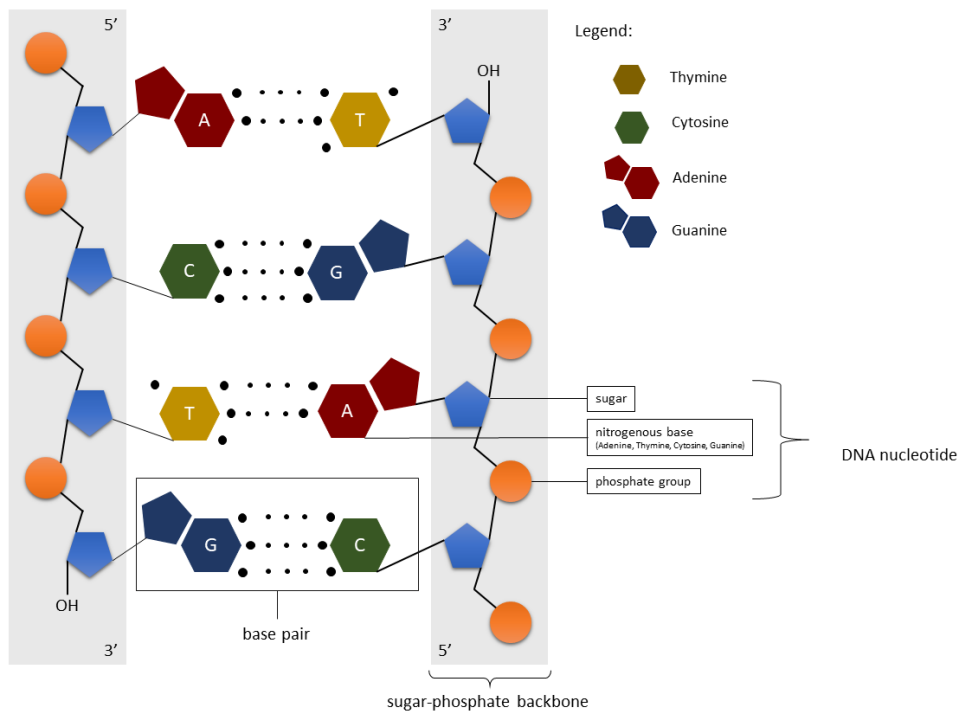


Figure 1. The DNA Structure and DNA composition

DNA Damage

The DNA needs to be protected as it is continually exposed to different DNA damaging agents, whether it be natural and man-made. DNA damage is any modification to the DNA coding properties or DNA transcription or replication. It can occur in varied forms including apurinic/apyrimidinic (AP) sites, adducts, single-strand breaks (SSBs), double-strand breaks (DSBs), DNA-protein cross-links, and insertion/deletion mismatches (Rao, Spring 1993).

Sources of DNA Damage

Every day, mammalian cells accumulate an estimated 100,000 lesions in their DNA as a result of factors such as replication stress, environmental genotoxins, exposure to reactive

oxygen species, and exposure to exogenous agents such as radiation e.g. ultraviolet and ionizing radiation, etc. (Figure 2).

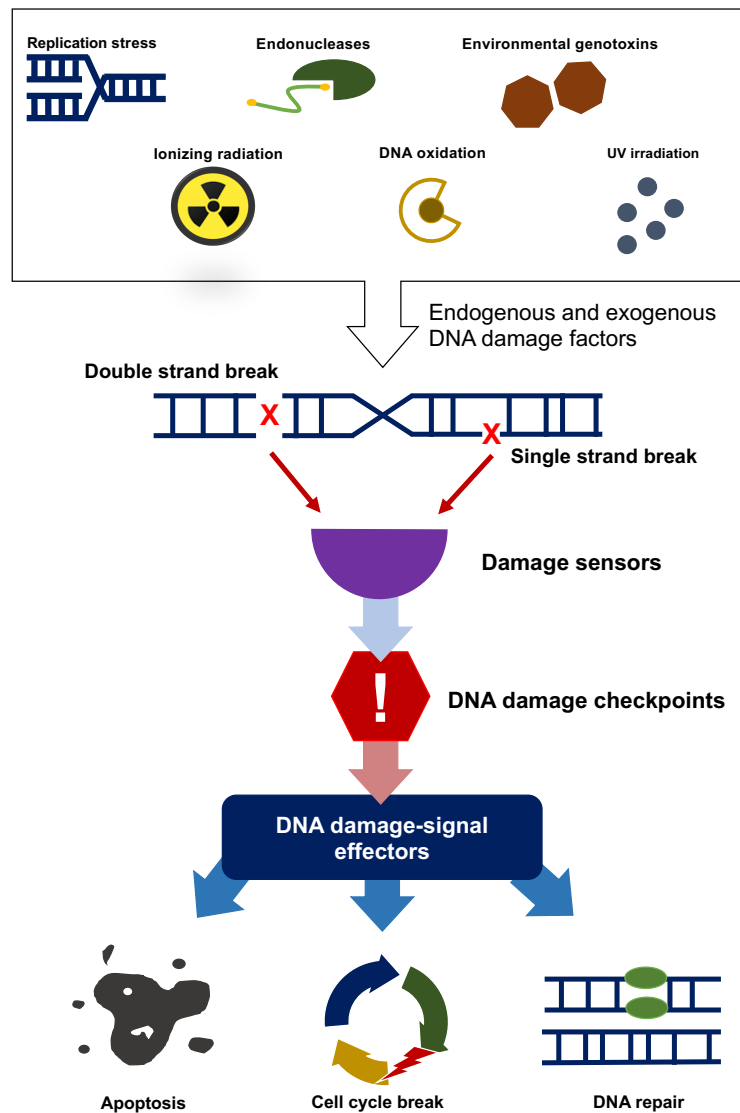


Figure 2. Sources of DNA Damage and Fate of DNA After Damage

Exogenic sources of DNA damage can be classified as physical source, or chemical source. Physical sources are radiation including UV radiation from the sun and ionizing radiation. UV radiation produces covalent bonds that crosslink adjacent pyrimidine bases in the DNA strand. Ionizing radiation initiates DNA mutations by generating free radicals within the cell that create reactive oxygen species (ROS) and result in single-strand and double-strand

breaks in the double helix. Chemical sources, on the other hand, can attach alkyl groups covalently to DNA bases or nitrogen compounds that can methylate or ethylate the DNA base. Endogenic sources of DNA damage are from DNA polymerases in processes such as DNA replication or from hydrolysis, oxidation, alkylation, and mismatch of DNA bases (Rask, et al., 2007) (Yu, et al., 2003).

Radiation and DNA Damage

Radiation is an energy that passes from a source through a certain space, which may be able to penetrate to certain materials. Radiation is both harmful and beneficial, hence the comparison to a two-edge sword. With the many beneficial effects especially in medical and diagnostic use for human health, it can also cause harm and is a possible carcinogen. Living organisms may be exposed to radiation in several ways such as medical and diagnostic procedures, exposure to background radiation from cosmic rays, natural radiation and radioactivity, nuclear tests, and nuclear accidents (Desouky, et al., 2015). When cells are exposed to radiation, the probability of the radiation interacting with the DNA molecule is very small because the DNA constitutes only a small part of the cell. However, the big portion of the cell which is water has a high probability of interaction with radiation. When radiation interacts with water, it can break bonds that hold the water molecule together, producing fragments such as hydrogen and hydroxyls which may be harmful or not depending on the ions and compounds that was created. However, when they could combine to form toxic substances, such as hydrogen peroxide (H_2O_2), this may contribute to indirect destruction of the cell. The degree of effect caused by ionizing radiation will also be dependent on other factors such as radiation dose, dose rate, type of radiation, the part of the body exposed, age, and health.

For ionizing radiation, radiochemical damage on the DNA can occur by direct or indirect action. If radiation interacts with atoms of the DNA molecule, or some other cellular

component critical to the survival of the cell, it is referred to as a direct effect. Such an interaction may affect the ability of the cell to reproduce and survive. This may cause an effect such that chromosomes may not replicate properly, or the information carried by the DNA molecule may be altered. Direct action may also cause one or both sugar phosphate backbones or the base pairs of the DNA to break physically.

In the mammalian cell, ionizing radiation induces around 850 pyrimidine lesions, 450 purine lesions, 1000 single-strand breaks (SSB) and 20–40 double-strand breaks (DSB) per cell per Gray with low linear energy transfer (LET) γ -radiation (Lomax, et al., 2013). A dose of 2 Gy/fraction of ionizing radiation which is a typical therapeutic dose may bring about 3000 DNA lesions per cell exposed (Lomax, et al., 2013). The most deleterious lesion induced by ionizing radiation is the DSB. The yield of DSB increases linearly with radiation dose, which starts from few mGy of radiation dose exposed (Rothkamm, et al., 2003).

The adverse effect of radiation can be categorized to deterministic and stochastic effects. Deterministic effects are characterized by a threshold dose in which below it, there is no clinical effect, and with increasing dose, the severity of certain effects to human body also increases (Desouky, et al., 2015). Stochastic effects on the other hand are associated to long-term, low-level chronic exposure to radiation. The probability of stochastic effects increases with radiation dose, but no threshold dose is assumed (Desouky, et al., 2015).

Radiation and Cell Survival

A cell survival curve shows the relationship between the radiation dose and the proportion of cells that survive. When cell loses its reproductive integrity, or its ability to proliferate indefinitely, it is considered to have undergone cell death. The mean lethal dose for loss of proliferative capacity in cells is usually less than 2 Gy, although a much higher dose, a dose of 100 Gy is necessary to significantly destroy cell function in nonproliferating systems.

A dose-survival curve is the loss of reproductive integrity as a function of radiation dose which may be assessed by the ability to form a colony which can be seen easily with the naked eye (Hall and Giaccia, 2012).

There are three models that mathematically describe cell survival curves: the single-target model, the multitarget model and the linear–quadratic (LQ) model. In the single-target model, the cell has a single target that when hit which causes the cell to die without an opportunity to repair the damage from radiation. The multitarget and LQ models are both considered multiple-target models which assume that the cell contains two or more targets that must be hit before the cell is killed. To be killed, the cell must accumulate enough targets in a limited time such that repair mechanisms are not capable to act. However, when the first target happens, the cell may have enough time to repair the damage before the next target, which is called sublethal damage. Low dose causes mostly sublethal damage, and high dose causes lethal damage. This may explain the change in slope, called a shoulder in a survival curve (Kelsey, et al., 2014).

There is a difference of the shape of survival curve depending upon the type of radiation. At “low doses” for sparsely ionizing or low-linear energy transfer [LET] radiation such as x-rays, the survival curve starts out straight on the log-linear plot with a finite initial, with a surviving fraction that is in exponential function of dose. At higher doses, the bending or curving region occurs which extends over a dose range of a few grays. Then at high doses, the survival curve often tends to straighten again, and the surviving fraction returns to being an exponential function of dose (Hall and Giaccia, 2012).

DNA Repair

To ensure faithful replication and transfer to daughter cell of DNA, multiple mechanisms have evolved to detect and counteract possible DNA lesions that may threat

genome integrity. Cells have developed multiple repair mechanisms wherein each corrects a different subset of lesions to repair damage. As a result, not all damages are irreversible, though in many instances, the cells are able to completely repair any damage and function normally. Some major DNA repair mechanisms are base excision repair (BER) which repairs damage to a single base; mismatch repair (MMR) which repairs mis-repaired but undamaged nucleotides; nucleotide excision repair (NER) which repairs bulky, helix-distorting lesions; and double-strand break (DSB) repair which includes both homologous recombination (HR) and End Joining (EJ) or more popularly known as non-homologous end joining (NHEJ). Other than the DNA repair pathway, cells have also developed DNA damage sensors, checkpoints, and signal effectors as control mechanisms in the cell cycle to signal for DNA repair and keep the integrity and fidelity of the cell. When cells are unsuccessfully repaired or the damage is critical, different consequences may occur such as cell-cycle arrest, apoptosis or cell death, and mutagenesis which may induce progression of diseases like cancer, aging, inborn diseases (Figure 2).

Double-Strand Break (DSB) Repair

Double-strand breaks in DNA occurs or arises when both strands of the DNA duplex are severed. It can result in loss and rearrangement of genomic sequences. Unrepaired DSBs are the most important lesions in inducing chromosomal abnormalities and gene mutations (Ward, 1995). The proper repair of DNA double strand breaks (DSBs) is vital for the preservation of genomic integrity. There are two main pathways that repair DSBs, Homologous recombination (HR) or template-assisted repair and Non-homologous end-joining (NHEJ) (Wang, et al., 2013), although current studies have also reported on the alternative end joining pathways of DSB repair (DiBiase, et al., 2000) (Dueva, et al., 2013) (Wang, et al., 2013) (Terzoudi, et al., 2000) (Chang, et al., 2017).

Non-Homologous End-Joining (NHEJ) Pathway

In mammalian cells, non-homologous end-joining (NHEJ) is the principal pathway for DSB repair throughout their entire cell cycle. There are several proteins which are reportedly involved in this pathway as shown in Figure 3. NHEJ begins with the binding of one heterodimeric protein called Ku70/80 to each end of the DSB to maintain them close together in preparation for ligation and prevent their degradation. Ku 70/80 forms a Ku: DNA complex with the DNA where the Ku heterodimeric protein positions the two ends of the broken DNA strands for repair. With this positioning, DNA sequence information is lost in the process. Multiple enzymes are involved in the rejoining process, including PAXX, DNA ligase IV, XRCC4, and DNA-dependent protein kinase (DNA-PK). The Ku:DNA complex serves as a node at which the nuclease, polymerases and ligase of NHEJ can dock (Lieber, 2010). Ku80, XRCC4 and Ligase IV are the 'core' NHEJ factors as these proteins were conserved during evolution and are required for all known NHEJ reactions. Ku heterodimer binds to the broken DNA ends and forms a complex with DNA-PKcs. The ligase IV/XRCC4 complex ligates the processed ends with the help of XLF.

NHEJ deficiencies in mice are associated with impaired neurogenesis and growth delay (Gao, et al., 1998) (Gu, et al., 2000) (Frank, et al., 2000). Defective NHEJ also causes gross chromosomal aberrations, genomic instability, and lymphomagenesis (Difilippantonio, et al., 2000). In research in mice, when NHEJ genes are disrupted, the radiosensitivity of the cells (Okayasu, et al., 2000), as well as its immunodeficiency (Woodbine, et al., 2014) are compromised. This is because of the important role that NHEJ play not only in DNA repair but also in V(D)J recombination process, where immunoglobulin genes are rearranged to generate diversity in immune system. Furthermore, mice deficient for XRCC4 or LIG4 are embryonic

lethal, with severe growth retardation and failure in neurogenesis which shows that NHEJ is essential for growth and neurogenesis.

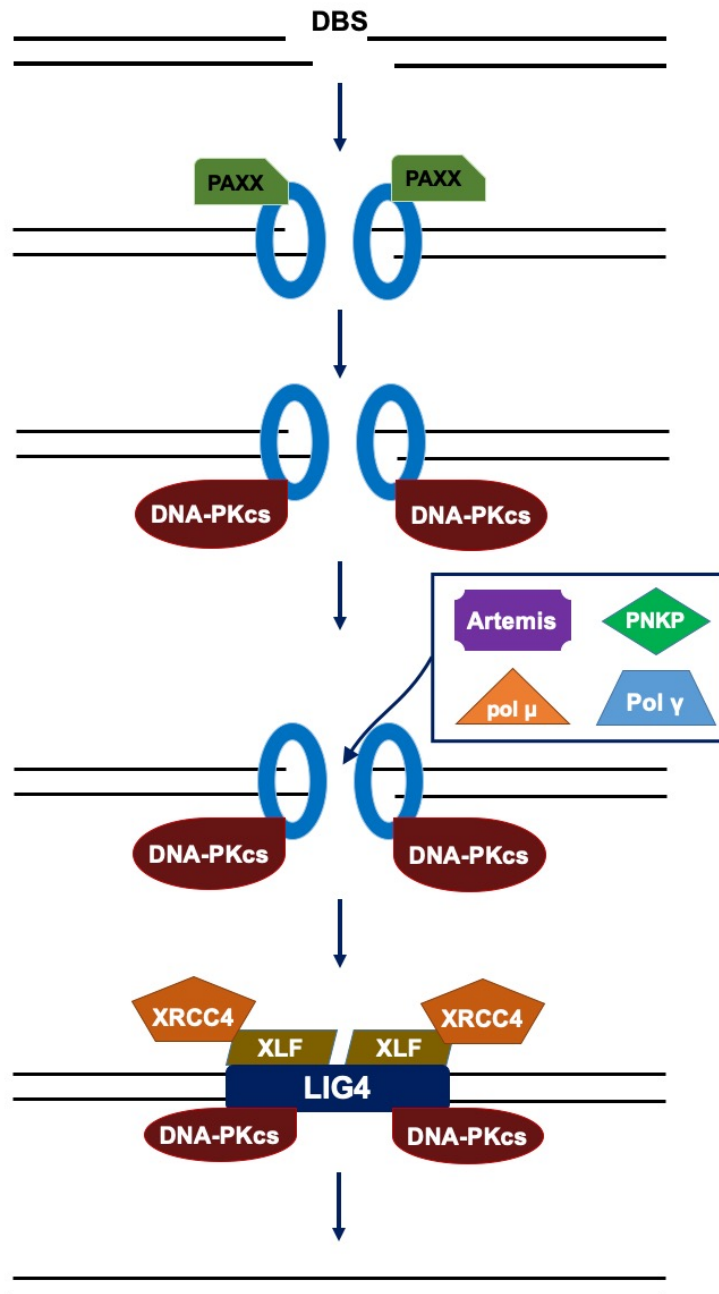


Figure 3. NHEJ Pathway and Proteins Involved in the Pathway

XRCC4

XRCC4 is a homodimer of 1008 nucleotides corresponding to 336 amino acids, which is responsible for the recruitment of several NHEJ factors to the DSB ends. The first subunit contains amino acid residues 1 – 203 and has a longer stalk than the second subunit which contains residues 1 – 178. Different important sites which allow for XRCC4 function are in different domains (Figure 4) which may be at the N-terminal, which is associated with its hydrophobic core, coiled coil where Ligase IV interacting domain is located and C-terminal domain where nuclear localization and phosphorylation sites are found.

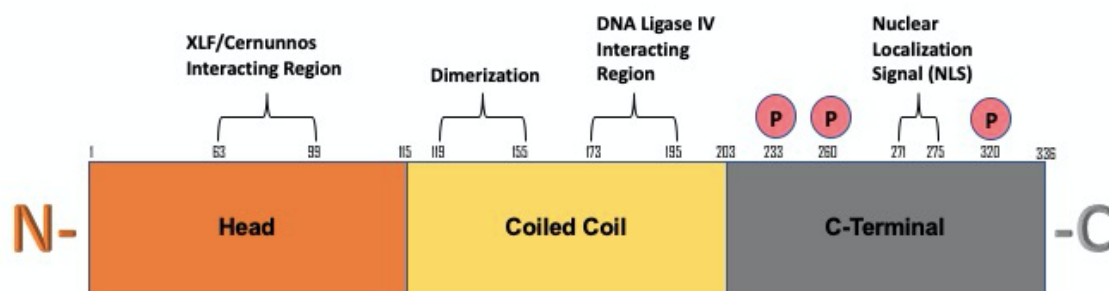


Figure 4. XRCC4 Structure and Location of Important Sites in Its Structure

XRCC4 has no known enzymatic activity, however, the best studied processing enzyme that XRCC4 interacts with is DNA ligase IV wherein XRCC4 is the key protein that enables interaction of ligase IV to damaged DNA and therefore ligation of the ends. XRCC4 tightly associates with Ligase IV to stabilize Ligase IV from degradation and to stimulate its action (He, et al., 2014). XRCC4 also binds DNA to DNA ligase IV (LIG4). XRCC4 tetramer bridges the two ends of the broken DNA and catalyzes the coordinate ligation of the two DNA strands (Lee, et al., 2000).

The LIG4-XRCC4 complex is responsible for the NHEJ ligation step, and XRCC4 enhances the joining activity of LIG4. Figure 5 shows the overall architecture of the XRCC4 in a homodimer in a complex with Ligase IV. The XRCC4 dimer is drawn as a ribbon where the head domains are blue; the helical tails, red; and the ligase-binding region, magenta. The ligase linker sequence is shown as a green tube. N- and C-termini are indicated for XRCC4 protomer A and for the ligase chain (Sibanda, et al., 2001).

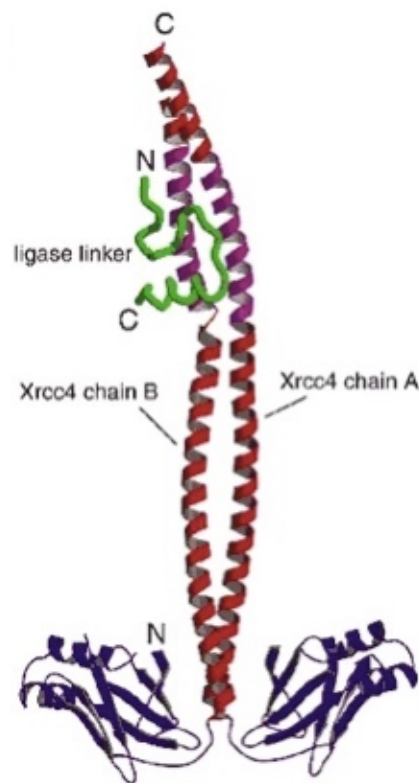


Figure 5. Overall Architecture of XRCC4-Ligase IV Complex (Sibanda et al. 2001)

XRCC4 is also in conjunction with the protein Ku for mediating the recruitment of processing enzymes to DSBs. Binding of the LIG4-XRCC4 complex to DNA ends is dependent on the assembly of the DNA-dependent protein kinase complex DNA-PK to these DNA ends. Because of the complex role of XRCC4 in NHEJ more than just basic recruitment of the terminal ligase for the repair of the DSB, mutations in the XRCC4 gene have been reported to

cause embryonic lethality in mice and developmental inhibition and immunodeficiency in humans. XRCC4 therefore has significant roles in NHEJ repair signaling and genomic integrity.

Genetic knock-out of XRCC4 in mice leads to embryonic death, which suggests that XRCC4 is critical for DSB repair during development (Gao, et al., 1998). Studies in mice showed that the deficiency in XRCC4 as well as LIG4 causes late embryonic lethality, associated with defective lymphogenesis and neurogenesis (Frank, et al., 2000) (Shaheen, et al., 2014).

XRCC4 Mutations Associated to Development

Mutations in the XRCC4 gene have been identified through whole-exome sequencing (WES) of patients with developmental diseases such as microcephaly and growth defects. These disease patients were found to harbor mutations on the DNA repair protein in XRCC4 (Bee, et al., 2015; de Bruin, et al., 2015; Guo, et al., 2015; He, et al., 2014; Murray, et al., 2015; Rosin, et al., 2015). Cells of these patients with different kinds of mutations at different locations of XRCC4 have caused varied effect in DNA repair from less or unstable XRCC4 expression to total loss of DNA repair function. Unexpectedly, however, the lymphocytes of most of these patients were reported to show normal immune levels, indicating normal immunological functions.

XRCC4 Mutation Associated to Increased Cancer Risk

There has been increasing interest in the role that DSB repair genes play in both cancer susceptibility and tumor development. XRCC4 has an important role in the non-homologous end joining pathway of DNA repair to maintain genome stability and for non-

occurrence of diseases like cancer. In a case-control study with breast cancer patients, the mutation A247S in XRCC4 is associated with breast cancer susceptibility in Chinese women and was identified as a breast cancer susceptibility gene in the Chinese population (He, et al., 2014). In another report on the XRCC4 247 polymorphism, this A247S polymorphism decreased survival and increased death risk of Diffusely Infiltrating Astrocytoma (DIA) which is a common tumor in the central nervous system (Lin, et al., 2013). There are other reports on XRCC4 single-nucleotide polymorphisms (SNPs) which were associated to hepatocellular carcinoma (Long, et al., 2013), lung cancer (Yu, et al., 2011), multiple myeloma (Cifci, et al., 2011), and oral cancer (Tseng, et al., 2008). When XRCC4 mutation occurs, there is a possibility of functional changes, thereby decreasing NHEJ capacity which may play an important role in the tumorigenesis. Because of this, an important research question established was the role of these XRCC4 mutations to the functions of XRCC4 in DNA repair ability through NHEJ pathway as well as in genomic stability to know the role of XRCC4 in cancer predisposition.

1.2 Statement of the Problem

Although the function of XRCC4 to NHEJ Pathway of DNA repair has been extensively studied, the extent of the role that disease mutations play to XRCC4 function in DNA repair has not yet been fully revealed. In this study the functional characteristics of XRCC4 mutations associated to development and cancer risks are analyzed to further delve into the significance of the XRCC4 structure in the role it plays in NHEJ, DNA Repair, tumorigenesis, genome stability and non-progression of diseases.

1.3 Objectives of the Study

This study aims to explore the role of XRCC4 in development and cancer suppression. Specifically, it aims to:

1. Introduce different mutations to the XRCC4 protein based on mutation of patients associated to development and cancer risks;
2. Analyze DNA repair function of XRCC4 mutated cells associated to development which are located at different positions in the XRCC4 gene;
3. Analyze the role of XRCC4 to cancer risk by comparing wild-type XRCC4 function to the functions of an XRCC4 polymorphism related to cancer and;
4. Determine the significance of the structure integrity of XRCC4 to its function in DNA double strand break as well cell stability and survival.

1.4 Significance of the Study

Mutations in XRCC4 identified with patients with development and cancer risks showed varied effects in DNA repair capability. In this study, some of the XRCC4 mutations associated with development and cancer risks reported in literature will be introduced to wild-type XRCC4 and analyzed with its functional characteristics to delve deeper to the function of the structure and the significance of the integrity of XRCC4 in the DNA repair and non-occurrence of diseases. Mutations to XRCC4 reported to be associated to development and cancer risks will be generated and its effect to DNA repair will be investigated by analyzing subcellular localization, functional characteristics, protein expression, DNA repair and radiosensitivity.

This research is significant because related studies mainly described the identification of the disease patients with various XRCC4 mutations. Some of them studied the functionality of XRCC4 in terms of DNA repair ability and radiosensitivity, but not all of these mutations were analyzed in these aspects. This is the first study to examine the functionality of various XRCC4 mutations in the same background. This study will give a better understanding on the characteristic of XRCC4 as a DNA repair protein in human and find out the effect of different

specific mutations to cell survival, and the potential role of specific mutations of XRCC4 to DNA repair function.

1.5 Scope and Delimitation

In previous studies, individual reports showed XRCC4 mutations after sequencing of the whole genome of patients. Because of the differences in the genetic make-up of each patient and the existence of multiple mutation to some patients, the effects of these mutations to the structure of XRCC4 and its functionality may not yet be fully revealed. In this study, instead of studying the fibroblasts of patients that harbor the mutations, these reported mutations are prepared in the same background as stable mutated transfectants from wild type-XRCC4 and are analyzed and compared in terms of their biochemical characteristics and effect in DNA repair, then allowing the comparison of different mutations of XRCC4 in terms of their function as compared to wild-type, normal functioning XRCC4 in the same genetic background.

The research is limited to the study of some but not all XRCC4 mutations reported to be associated with developmental diseases and cancer risks, successfully generated during the current study. It is also limited only to in vitro studies of the mutations and not to the cells obtained from the fibroblasts of the patients directly.

Lastly, in this study, the radiosensitivity of different mutations was shown without showing the radiosensitivity of threshold dose, due to the fact that even if it is present, threshold is below 100 mSv or 0.1 Gy. This threshold for 0.1 Gy cell survival maybe far smaller than dose studied for radiosensitivity in this research which is 2 and 4 Gy. It is expected that the radiosensitivity of the threshold if ever studied and included, will be very close to 1 which maybe difficult to discern from unirradiated cells and maybe within statistical variation.

1.6 Definition of Terms

Conceptual Definition:

Frameshift Mutation– mutation that occurs when the addition or loss of DNA bases changes a gene's reading frame, shifts the grouping of the bases and changes the code for amino acids.

Point Mutation – mutation in the form of insertion, deletion or substitution to a single nucleotide base in a sequence of DNA or RNA

Microcephaly - head circumference measurement that is smaller than a certain value for babies of the same age and sex, usually more than 2 standard deviations (SDs) below the average.

Missense mutation –a point mutation in which a single nucleotide change results in a codon that codes for a different amino acid

Nonsense mutation – a genetic mutation in a DNA sequence that results in a shorter, unfinished protein product.

Operational Definition:

A247S – substitution of Alanine to Serine at position 247

D254Mfs*68 – Substitution of aspartic acid (D) to Methionine causing a frameshift of 68 nucleotides; 68th codon is a stop codon.

R161Q – substitution from Arginine to Glutamine at position 161

R225X – deletion of Arginine at position 275 causing a premature stop to XRCC4 sequence.

R275X – deletion of Arginine at position 275 causing a premature stop to XRCC4 sequence.

W43R – substitution from Tryptophan to Arginine at Position 43

V83_S105del – deletion from Valine at Position 83 to Serine at position 105 causing deletion of 23 amino aci

Chapter 2. Materials and Methods

Chapter 2

Materials and Methods

2.1 Cell Culture and Subculture

Murine M10 L5178Y-derived Leukemia Cell Line (M10) obtained from RIKEN cell bank (Tsukuba, Ibaraki, Japan; Code RCB0136) were cultured in RPMI1640 medium supplemented with 10% fetal bovine serum (FBS) and 1% penicillin (5000 µg/ml) - streptomycin (5000 µg/ml) and 100 µl 1 % Beta-mercaptoethanol mixed solution as antibiotics and allowed to grow in 25 cm² culture flasks in a humidified 5% CO₂, 37°C incubator. The cells were sub-cultured in a new culture flask with fresh culture medium every 3-5 days to ensure healthy growth which is characterized by smooth, round appearance of the cells.

Human Osteosarcoma cell line (U₂OS) was cultured in DMEM/Ham's F2 medium (NacalaiTesque, Kyoto, Japan) supplemented with 10% FB (Hyclone, Logan, UT, USA), 100 units/mL penicillin (NacalaiTesque, Kyoto, Japan) and 100 µg/mL streptomycin (NacalaiTesque, Kyoto, Japan) at 37°C in humidified atmosphere containing 5% CO₂.

Cultured cells proliferate in a standard growth pattern. After the cells are seeded, the growth of the cells is in the lag phase when the cells are adapting to their new environment and preparing for fast growth. Log phase is the period of fast growth after lag phase when cells proliferate exponentially and consume more nutrients in the culture medium. When the culture medium starts to be depleted of nutrients or when the available spaces are filled up, the growth phase is said to be stationary or in a plateau, when proliferation is greatly reduces and starts to cease. For optimal growth, cells require enough space for expansion, and enough nutrients to grow. Therefore, there is a need to subculture in new culture flasks with fresh culture medium.

As M10 cells are suspension cells which doesn't adhere to container, the subculture can be done by diluting the cells 20-30 folds in a new flask with new culture media. M10 cells are

passaged every 2-3 days during the log phase before they reach confluency. For attached U2OS cells needs to be detached before dilution. The cells are washed with phosphate-buffered saline PBS (-) twice and then enzymatically treated with Trypsin to detach them from the surface of culture dishes. After ensuring detachment, cells are centrifuged, and diluted to desired confluency in a new culture dish with new culture medium.

2.2 Freeze Stock and Thawing frozen cells

Cells which are continuously cultured are prone to microbial contamination and senescence, so preserving them for long storage is a must especially when dealing with established cell lines. It also prevents the cell aging when passing through several generations of passaging to maintain the minimal number of generations from initial stock. Freeze stocks are stored in -85 degrees Celsius and can be thawed when needed. To prepare a freeze stock, cells were harvested by centrifugation at 1000 rpm for 5 minutes and supernatant was removed. Cell pellets were mixed with freezing media to a final concentration of 10^6 cells/ml. When needed to be thawed, frozen cells are thawed rapidly at 37 degrees Celsius water bath. Thawed cells were then diluted in culture medium and centrifuged at 1000 rpm for 5 minutes to remove the previous supernatant which is toxic at room temperature. Then, thawed cells were suspended in new culture media and kept in 37 degrees Celsius incubator for optimum growth.

2.3 Mutagenesis

Vector

Stable Transfection

In this study, two types of vectors were used. The first vector as shown in Figure 6 is the p3xFLAG-CMV10 vector which is a shuttle vector for Escherichia coli and mammalian

cells where the normal human XRCC4 cDNA and the different mutations are inserted. The p3xFLAG-CMV10 vector has neomycin resistance as well as ampicillin resistance for growth selection in bacterial and mammalian cells. The main advantage of p3xFLAG-CMV10 vector is that it contains strong CMV promoter for high level expression in mammalian cells, and p3xFLAG which is three times Flag tag which enhances the detection of low expression proteins.

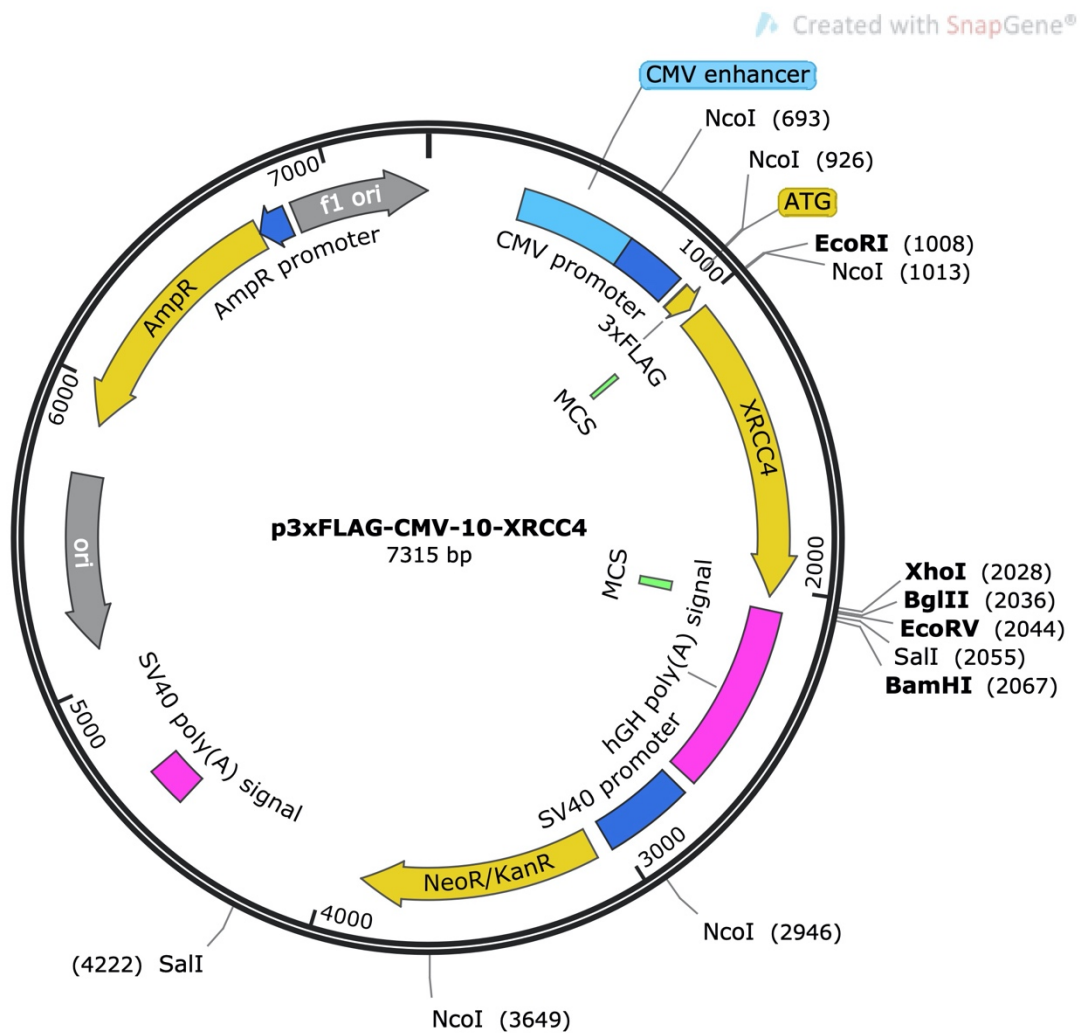


Figure 6. PCMV10 Vector Map

Transient Transfection

Another vector used in this study is the pEGFP-C1 as shown in Figure 7, which was used as vector for the constructs of mutations of XRCC4 in several analysis such as subcellular localization. pEGFP-C1 encodes for a red variant of wild-type GFP has been optimized for higher expression in mammalian cells as well as brighter fluorescence for improved microscopy. pEGFP-C1 also contains neomycin and kanamycin resistance which allows for selection of stable transfected eukaryotic cells.

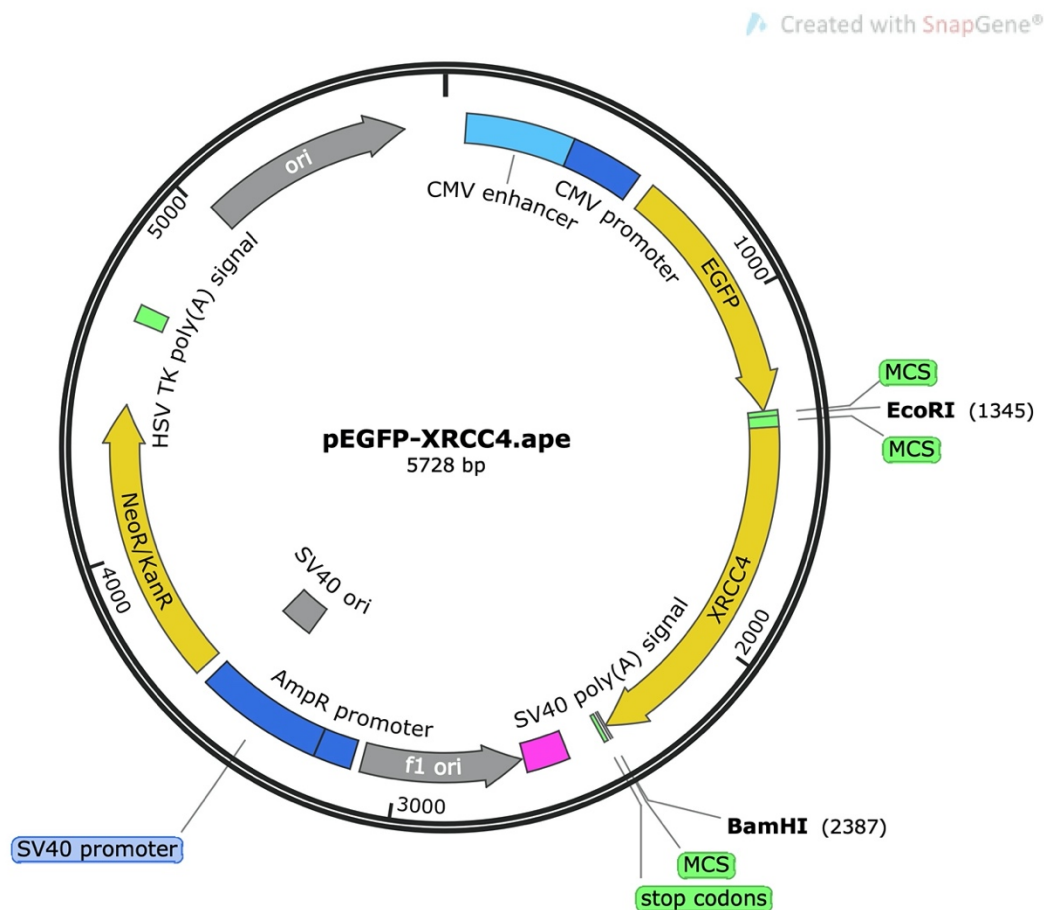


Figure 7. pEGFP-C1 Vector

Primer Design

To produce the desired mutations in the XRCC4 gene, the right primer is necessary to successfully amplify the DNA. To design the primer, the codes corresponding to the mutation were placed in the middle of the sequence being generated. Eighteen (18) nucleotides, the same as the original wild type XRCC4 sequence, were copied and added before and after the position of the mutations for both the 5'- and the 3'- ends. These primer designs were requested to be generated to the company. Primers were then obtained, and plasmids are constructed using the primer design for each of the mutations.

Table 1. Forward and Reverse Primer Sequences for the generation of XRCC4 mutations based on patients associated to diseases in development and cancer risks

XRCC4 Mutation	Forward and Reverse Primer Sequence
W43R	Forward: 5-TCAGCACGGACTGGGACAGTTTCTGAA-3
	Reverse: 5-CCCAGTCCGTGCTGAATGACCATCAGT-3
V83S-105del	Forward: 5-GCTGATTTTCAGACTTGGTTCCTTC-3
	Reverse: 5-TCTGAAATCAGCTGGTCCTGCTCC-3
R161Q	Forward: 5-CAAGGACAATTTGAAAAATGTGAGT-3
	Reverse: 5-TTCAAATTGTCCTTGAACATCATTCCA-3
R225X	Forward: 5-GCTGACTGAGATCCAGTCTATGATGAG-3
	Reverse: 5-TGGATCTCAGCAGTCATTTCAGA -3
R275X	Forward: 5-AGACAGTGAATGCAAAGAAATCTTGG-3
	Reverse: 5-TTGCATTCACTGTCTCCTTTTTTCTACT-3
D254Mfs*68	Forward: 5-AGTAAAATGATTCCATTATTTCAAGT -3
	Reverse: 5-GGAATCATTTTACTTACAGCAGCTGA-3
A247S	Forward: 5-GGGTTGTCTTCAGCTGTCGTAAGTAAA -3
	Reverse: 5-AGCTGAAGACAACCCAGAGAGATCAGT-3

Plasmid Construction

Plasmids were inserted to the p3xFLAG-CMV10 vector by polymerase chain reaction (PCR) using PrimeSTAR Max Premix (2X), and forward primer and reverse primer with a final concentration of 0.2 μ M plasmid concentration. Deionized water was mixed to make a final volume of 10 μ L sample for each mutation sample. The PCR tubes were placed inside the PCR Thermal cycler Dice (TaKaRa, Japan) with conditions as shown in Table 2. After this step was performed, PCR products of mutated XRCC4 were contained in the plasmid.

Table 2. Conditions for the Polymerase Chain Reaction (PCR) For the Insertion of the XRCC4 Mutations to the Plasmid

PCR Steps	Temperature	Time
Initialization	98°C	3 minutes
Denaturation	98°C	10 seconds
Annealing	55°C	15 seconds
Elongation	72°C	30 seconds
Elongation	72°C	6 minutes
Final Hold	4°C	Indefinite

Bacterial Transformation

The plasmids were introduced to bacteria cells by transformation. In the process of transformation, lysogeny broth (LB) plates were used for the bacteria to grow. First, the LB plates were prepared by combining 2.5% w/v LB broth with 1.5% w/v agarose in deionized water. The mixture was autoclaved at 121°C for about 121 minutes and left to cool down about 65°C before the antibiotic Ampicillin (50 μ g/mL) was added for the purpose of selectively

excluding *Escherichia coli* without the exogenous DNA. This solution was poured in plates and allowed to solidify.

Competent cells (E coli HIT-JM-109) from -80°C freezer was thawed by dipping in room temperature water for 10 seconds. About 10% v/v plasmid was added in 20 µL aliquot of *Escherichia coli* competent cells and placed on ice for 10 minutes. A one-minute heat shock was performed to the bacterial solution to enhance uptake of exogenous DNA into *Escherichia coli*. The plasmid-bacterial solution was put back in ice for 10 minutes before plating in LB plate and then incubated at 37°C overnight.

Proliferation of Competent Cells

Colonies were formed in LB plate when the plasmid were successfully inserted in the competent cell. A single colony was picked and placed in 15 mL centrifuge tube containing 3 mL of LB medium (2.5 % w/v LB broth powder in deionized water added with 30 µg/mL Kanamycin. The tubes were placed in a shaker incubator at 37°C and 180 rotations/minutes to proliferate the *Escherichia coli* overnight.

DNA Purification

MINI Prep protocol was used to isolate high copy plasmid DNA from the *E.coli*. Briefly, *Escherichia coli* cells are cultured in 15 mL centrifuge tube overnight. Then the cell culture was transferred to a 1.5 mL tube and centrifuged at 16000g for 1 minute to collect cell pellets. The centrifuge tube is then vortexed to break cell pellets. Then several kinds of lysis buffer from the Mini Prep Kit was used to treat the cells. After treating with buffers, the solution was centrifuged for 5 minutes to remove any sediments that formed after reaction. A column and collection tube were used to load the supernatant and then centrifuged again wherein the flow-through was disposed. The column was then washed with wash buffer and centrifuged again

to remove any remaining buffer. Elution buffer was then used to treat the cells and collect the plasmid DNA. The concentration of the plasmid was measured using Nanodrop ND-1000 spectrophotometer.

MIDI/MAXI Prep Protocol was used to purify large concentration of plasmid DNA. The MIDI Prep Kit utilizes a Nucleosome Extra Silica Resin to purify plasmid DNA. The DNA which is negatively charged can bind with the positively charged anion exchanger group in the resin. Cells for MIDI/MAXI Prep are cultured in 200 mL flask overnight and transferred to large centrifuge bottles. A high-speed centrifuge machine was then used for large volume centrifugation. After centrifugation, the cell pellet was then vortexed repeatedly to allow to disintegrate. Buffers were then added to lyse the bacteria cells. The lysate was loaded to Nucleobond Xtra Column Filter equilibrated with buffer. The plasmid DNA was collected by the resin in the column. After discarding the filter and washing again with buffer, the resin was washed with another buffer and the DNA is eluted from the resin with an elution buffer. The eluate is mixed with isopropanol and reconstituted using the Nucleobond Finalizer from the kit, and Tris buffer. The concentration of the plasmid was measured using NanoDrop ND-1000 spectrophotometer.

Restriction Enzyme Check

Restriction enzyme recognizes and cleave DNA double strand at specified nucleotide sequences. Insert check was performed to know if the plasmid of interest was inserted as a recombinant plasmid. The DNA was treated with restriction enzyme and loaded in electrophoresis gel containing 2.5% w/v agarose in 0.5 % Tris/Borate/Ethylenediaminetetraacetic acid (EDTA), or TRIS buffer. Electrophoresis was run for 30-45 minutes at 100 V. Successful insert checks show marked bands indicating pCMV vector and the XRCC4.

Sequence Check

The DNA was sent for sequence check to know if proper mutation is established before transfecting into mammalian cells. Sequence check samples were prepared containing 300-600 ng plasmid and 6.4 pmol universal primer in a final volume of 14 uL.

2.4 Transfection

Stable Transfection

To introduce the plasmid DNA to mammalian cells, stable transfection was performed into M10 cell line, an XRCC4-deficient derivative of murine leukemia cell line L5178Y, harboring a nonsense mutation in XRCC4 gene (c.A370T, p.R124X) (Mori, et al., 2001) (Sato, et al., 1979). M10 cells are mostly null functional due to the loss of interaction with Ligase IV. Transfection was performed by electroporation using Neon Transfection system (Invitrogen, Calsbad, CA, USA). About 10^6 M10 cells were transfected with 1 ug/mL plasmid DNA and allowed to grow in RPMI1640 medium with 10% fetal bovine serum in 24 hours. Transfected cells were then plated into 0.17% w/v agarose plate containing RPMI1640 medium supplemented with 15%FBS, 1% penicillin and streptomycin, 10 uM β -Mercaptoethanol and G418 with final concentration of 0.8 mg/mL. Once colonies were formed, they were picked up and cultured in culture medium for analysis.

Transient Transfection

For U₂OS cells, plasmids were transfected using Lipofectamine 2000 Reagent (Invitrogen). To knockdown endogenous XRCC4, small interfering RNA (siRNA targeting 3'- untranslated regions (UTR) was transfected 24 hours before plasmid transfection. The sequences of RNA duplexes were 5'- CUA UGU UUU CUA UUC AUU UdCdT -3' and 5' - AAA UGA AUA GAA AAC AUA GdTdC -3' where d is deoxyribonucleotide.

2.5 Analysis of Functional Characteristics of XRCC4 Mutations

Protein Expression Level

Sodium dodecyl sulfate polyacrylamide gel electrophoresis (SDS-PAGE), SDS-PAGE utilizes a gel with SDS which give a negative charge to each protein in proportion to mass. The SDS sample buffer consisted of 125 mM tris-hydroxymethyl aminomethane (Tris) (pH 6.8), 4 % w/v SDS, 20% v/v glycerol, 5% v/v glycerol, 5% β -mercaptoethanol, 0.05% w/v bromophenol blue and 0.01% w/v crystal violet. The gel utilized a combination of SDS separating gel solution containing 1.5 M Tris (pH 6.8), 0.4% w/v SDS, 10% acrylamide/bis-acrylamide (40:1), 0.1% v/v tetramethylethyene diamine (TEMED) and 0.03% w/v ammonium persulfate (APS) 1.5 M Tris, as well as SDS stacking gel solution at the top of the plate (about 2.5 cm from top of the plate) containing 0.5 M Tris (pH 8.8), 0.4% w/v SDS, 10% acrylamide/bis-acrylamide (40:1), 0.1% v/v TEMED and 0.075 w/v APS in between two glass plates with rubber strip and comb as shown in the figure. The gel plate was assembled into the gel cassette and the samples were loaded into the wells created by the comb. The current and voltage for electrophoresis was set to 20 mA per gel, and 200 V respectively.

After SDS-PAGE, western blotting was performed to detect protein of interest by probing specific antibody to a target protein. The electrophoresis gel utilized in SDS-page is removed in the gel cassette and gel plate to be transferred in a polyvinylidene difluoride (PVDF) membrane (Merck-Millipore, Billerica, MA, USA, 6 cm by 9 cm per gel). This membrane was pre-washed in methanol for one minute and stored in the transfer buffer (100 mM Tris, 192 mM glycine and 5% methanol until use. The transfer from gel to membrane utilized a transfer device set to 110V and 110 mA current per gel. The transfer also utilized filter papers of the same size of the membrane soaked in transfer buffer. The filter paper,

membrane and gel were utilized by placing three filter papers in the bottom most part of the transfer machine, followed by the membrane, and then the gel from SDS-PAGE, and lastly three more filter papers on top of the gel. Bubbles in between each layer which may hinder good transfer to membrane were removed using a roller before starting transfer at given voltage and amperes.

After the transfer step, blocking is needed to prevent membrane and antibody to interact which may cause noise. The blocking solution was 1% w/v skim milk diluted in a solution called TBST solution which consisted of 20 mM Tris (pH 7.6), 150 mM NaCl and 0,05% v/v Tween 20. Blocking was performed overnight.

After blocking, antibody (0.1% v/v antibody) was applied in the PVDF membrane. Anti-XRCC4 rabbit polyclonal antibody (Kamdar, et al., 2010), anti-FLAG mouse monoclonal antibody (clone M2; F3165; Sigma-Aldrich; St. Louis, MO, USA), anti-Glyceraldehyde-3-Phosphate Dehydrogenase (GAPDH) mouse monoclonal antibody (clone 6C5; MAB374;), and anti-LIG4 guinea pig polyclonal antibody (gifted by Prof. Miki Shinohara, Kinki University) were used as the primary antibody at 1/1000 to 1/5000 dilution. As the secondary antibody, horseradish peroxidase-conjugated anti-rabbit immunoglobulins swine polyclonal antibody (P0399; Dako; Glostrup, Denmark), anti-mouse immunoglobulins goat polyclonal antibody (P0447; Dako) or anti-guinea pig immunoglobulins rabbit polyclonal antibody (P0141; Dako) was used at 1/1000 to 1/3000 dilution.

The membrane was sealed and incubated with shaking for 30 minute or overnight. The membrane was washed 5 times with TBS-T solution (20 mM Tris (pH 7.6), 150 mM NaCl with 20% Tween 20) changing the TBS-T solution every other stop. After the membrane was probed with primary and secondary antibody, WesternSure Chemiluminescent Western Blot reagent (LI-COR; Lincoln, NE, USA) was used to develop the membrane and see the band formed in

the membrane which will correspond to protein size which was captured by captured by C-Digit Blot Scanner (LI-COR).

Nuclear Localization

Nuclear Localization was observed after transfection with GFP. Plasmids were transfected using Lipofectamine 2000 Reagent (Invitrogen). To knockdown endogenous XRCC4, small interfering RNA (siRNA targeting 3'-untranslated region (UTR) was transfected 24 hours prior to plasmid transfection. The sequences of RNA duplexes were 5'-CUA UGU UUU CUA UUC AUU UdCdT -3' and 5' - AAA UGA AUA GAA AAC AUA GdTdC -3' where "d" indicates deoxyribonucleotide. Subcellular localization GFP-tagged XRCC4 was observed two days after cDNA transfection using inverted fluorescence microscope IX71 (Olympus; Tokyo, Japan). Fluorescence of EGP was observed in inverted fluorescence microscope IX71 (Olympus; Tokyo, Japan). The nucleus of U2OS cells was stained with 4',6'-diaminodi-phenylindole (DAPI). The subcellular localization was quantified by counting 200-400 cells and identifying their localization in terms of whether it is found in the nucleus, nucleus and cytoplasm or cytoplasm only.

Radiosensitivity Analysis

Radiation Source

Cells were irradiated using ^{60}Co γ -source (222 TBq as of February 2010) . The dose rate was measured using ionizing chamber-type exposure dosimeter C-110 and the time to obtain the desired dose was calculated considering the ascending and descending of the delay time of the irradiation source. The Cobalt-60 source has an energy of 1.17 MeV and 1.33 MeV and a half-life of 5.27 years.

Colony Formation Assay

Colony Formation Assay is used to measure the ability of the cells to proliferate by forming colonies. This assay is used to analyze the effect of irradiation on the survival of the M10 cells with and without mutations. About 3.0×10^5 cells were counted and collected into 15 mL tube. The cells were then gamma-irradiated using Cobalt-60 source (half-life=5.27 years) with gamma energies 1.17 MeV and 1.33 MeV, at 2.0 and 4.0 Gy, with the exposure time calculated with consideration of dose rate and its decay through time of irradiation and the delay time of the irradiation source.

After irradiation, irradiated cells were diluted, and appropriate number of cells were mixed into plating media containing 0.17 % w/v agarose in RPMI1640 solution with 15% FBS and 1% penicillin and streptomycin and were then dispensed into 3 plates with maximum 1000 colonies per plate.

Surviving Fraction Analysis

Cells were allowed to grow for 12-14 days at the 5% CO₂, 37°C incubator after plating. To find out the number of cells that were able to withstand irradiation, the number of cells that appear in the plate were counted.

To compute for the surviving fraction, the formula is shown below:

$$\text{Plating Efficiency}$$
$$PE = \frac{\text{number of colonies counted}}{\text{number of cells plated}}$$

$$\text{Surviving Fraction}$$
$$SF = \frac{PE \text{ of irradiated cells}}{PE \text{ of non - irradiated cells}}$$

Immunofluorescence

About 10^5 cells were exposed to radiation of 2 and 4 Gray, and then were attached on a glass slide by centrifugation at 100g for 5 min. Cells were then fixed in the slides using 4% paraformaldehyde-containing phosphate-buffered saline PBS (-) and permeabilized with 0.5% Triton X-100-containing PBS(-). Slides were incubated with 5% bovine serum albumin-containing PBS (-) (BSA-PBS) for one hour at room temperature for blocking. Anti- γ -H2AX rabbit polyclonal antibody (Merck Millipore, 05-636) in BSA-PBS was used as primary antibody in which cells were treated overnight. After washing four times with 0.05% Tween 20-containing PBS (T-PBS), slides were incubated with secondary antibody, Alexa Fluor 594-conjugated anti-mouse IgG(H+L) goat polyclonal antibody (Invitrogen, A-11 032), which was used to treat cells for one hour at room temperature. After washing five times with PBS-T, slides were stained with 100 ng/ml of 4',6-diamidino-2-phenylindole dihydrochloride (DAPI) in Fluorescent Mounting Medium (DAKO) and observed using an inverted fluorescent microscope IX-71 (Olympus). Fluorescent images were analyzed using ImageJ software and γ -H2AX foci were automatically detected and enumerated. Statistical significance was determined using one-sided Welch's t-test.

Chromatin Binding Assay

About 10^7 CMV, XRCC4 and A247S cells were harvested and rinsed twice with ice-cold phosphate-buffered saline (PBS). The cell pellet was suspended in 150 μ l of buffer A (50 mM HEPES-NaOH (pH 7.5), 150 mM NaCl, 1 mM EDTA, 1/100 volume each of protease inhibitor cocktail for animal cells (Nacalai Tesque), phosphatase inhibitor cocktail I and II (Sigma-Aldrich)) with 0.2% Nonidet P-40. After standing on ice for 5 min, the suspension was centrifuged at 1,000 xg for 5 min and the supernatant was recovered as F-I. The cell pellet, was

resuspended in 150 μ l of the same buffer and immediately centrifuged at 1,000xg for 5 min. The supernatant was recovered, was then resuspended in 150 μ l of buffer A with 0.5% Nonidet P-40. After standing on ice for 40 min, the suspension was centrifuged at 16,000 xg for 5 min and the supernatant was recovered. The resultant pellet was suspended in equivalent volume of 2xSDS-PAGE loading buffer and heated in boiling water for 5 min. After centrifugation at 16,000 xg for 5 min, the supernatant was recovered as F-IV.

Laser Micro-irradiation

GFP-XRCC4 stably expressing U2OS cells were plated on the glass-bottom 35 mm dishes and transfected with siRNA 2 days before observation. At the day of observation, culture media were replaced with phenol red-free DMEM (Nacalai Tesque Inc.) supplemented with 10 % FBS. Then about 0.5 μ g/mL Hoechst 33342 (Dojindo Molecular Technologies, Inc.) was added 30 minutes prior to the observation to sensitize the DNA damage. Leica TCS SP8 LIGHTNING Confocal Microscope (Leica microsystems) with a 63x/1.40 oil immersion objective lens was used for induction of localized DNA damages by laser micro-irradiation. For the quantification, 20 cells were irradiated with laser, and then the intensity of green fluorescence was analyzed. The green fluorescence intensity at the irradiated sites were converted into numerical values by using SP8 software (Leica microsystems). The relative green fluorescence intensity was acquired after subtraction of the background intensity in the cells and division by the intensity at the irradiated area.

Computational Analysis

Dynamut was used as the program for analysis and prediction of protein stability changes upon point mutation using Normal Mode Analysis. By using Dynamut, Delta Delta G (DDG) can be computed which is a metric for predicting how a single point mutation will affect protein

stability. $\Delta\Delta G$, or $\Delta\Delta G$, is the change in the change in Gibbs free energy, and is a measure of change in energy between the folded and unfolded states (ΔG) and change in ΔG when point mutation is present. This folding has been found to be an excellent predictor of whether a point mutation will be favorable in terms of protein stability. The information about the proteins were obtained from the Protein Data Bank (PDB) archive-information. The structures used in this study is the crystal structure of Human XRCC4 with PDB Accession Number 1FU1 and the structure of human XRCC4 in complex with the tandem BRCT domains of DNA Ligase IV with PDB Accession Number 3II6.

**Chapter 3. Analysis of the Functional Characteristics of XRCC4 Mutations Associated to
Development**

Chapter 3

Analysis of the Functional Characteristics of XRCC4 Mutations Associated to Development

3.1. Generation of Mutations in XRCC4 Associated to Development

XRCC4 mutations reported in literature to be associated to development are shown in Table 1 with its location in XRCC4 structure in Figure 8. All XRCC4 mutations are analyzed to be in different positions, varying in kind of mutation, with long deletions or substitution, and causing a change in corresponding amino acid, truncation of sequence or frameshift of the sequence. The different mutations may be near the N-terminal end, in the coiled coil region near the sequence encoding for dimerization of the protein, sequence for interaction with Ligase IV, in the nuclear localization signal sequences (NLS) or at the C-Terminal domain. Table 3 and 4 on the other hand shows summary of XRCC4 mutations and the associated developmental problems and diseases and the summary of patients profile associated to XRCC4 mutations, respectively. A more detailed patient profile is found in the appendix 1. As shown in Table 3 and 4, a common feature to these patients is microcephaly and short stature like features with other complications. The mutations can be homozygous mutation in the patient but heterozygous to another mutation in the XRCC4 structure.

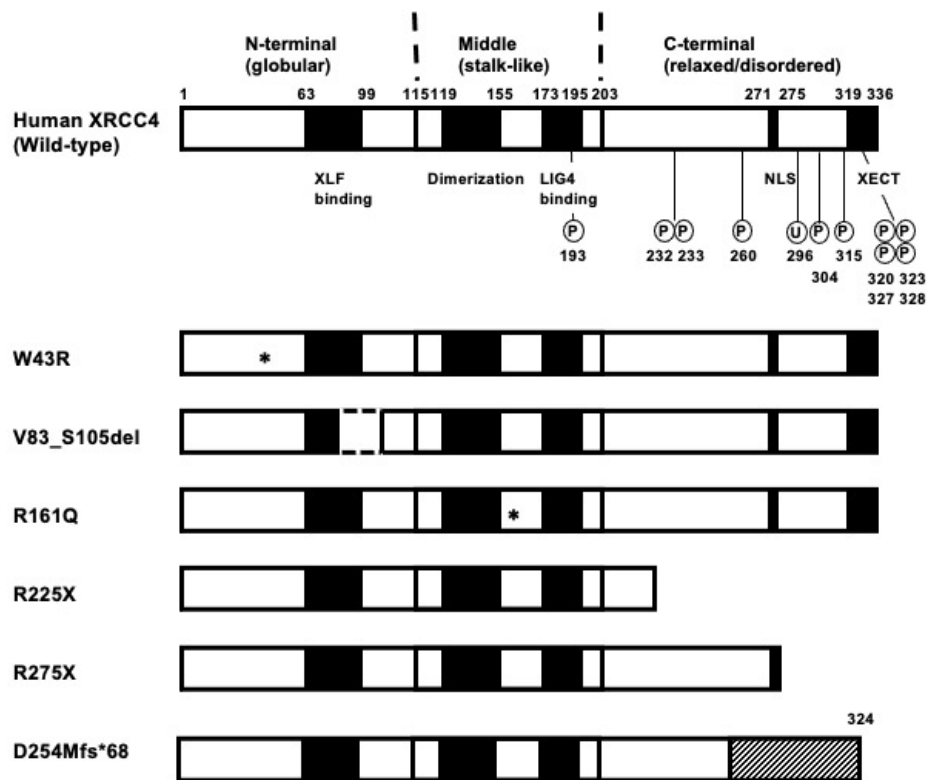


Figure 8. Location of XRCC4 mutation as compared to Wild-type XRCC4 structure

Table 3. Summary of XRCC4 Mutations Reported in Literature

XRCC4 Mutation	Diseases	Nucleotide Mutation	Status	Reference
V83_S105del	Microcephaly Severe Short Stature Primary Gonadal Failure Early-Onset Metabolic Syndrome Malignant Gastrointestinal Stromal Tumor	c.247_315del	Homozygous	(de Bruin, et al., 2015)
W43R	Microcephalic Primordial Dwarfism	c.127T>C	Homozygous Homozygous	(Shaheen, et al., 2014) (Murray, et al., 2015)
R161Q	Severe Microcephaly Facial Dysmorphism	c.482G>A	Homozygous	(Rosin, et al., 2015)

	Short Stature			
R225X	Microcephalic Primordial Dwarfism	c.673C>T	Heterozygous (+p.R161X)	(Murray, et al., 2015)
	Cardiomyopathy Neurological Syndrome Low Stature Depression Cognitive Impairment		Homozygous	(Bee, et al., 2015)
	Microcephaly Developmental Delay Progressive Ataxia Diabetes Mellitus Hypothyroidism Thalamic Glioma Moderate Hearing Loss Slurred Speech		Heterozygous (+p.D254Mfs*68)	(Guo, et al., 2015)
R275X	Microcephalic Primordial Dwarfism	c.823C>T	Homozygous	(Murray, et al., 2015)
	Severe Microcephaly Facial Dysmorphism Short Stature		Heterozygous (+His9Thrfs*8)	(Rosin, et al., 2015)
D254Mfs*68	Microcephaly Developmental Delay Progressive Ataxia Diabetes Mellitus Hypothyroidism Thalamic Glioma Moderate Hearing Loss Slurred Speech	c.G760del	Heterozygous (+p.R225x)	(Guo, et al., 2015)

Table 4. Profile of Patients Reported to be Harboring XRCC4 Mutations in Related Literature

Patient	Change in nucleotide sequence	Change in amino acid sequence	Clinical features			Reference
			Microcephaly (OFC)	Short stature (Length/height)	Other features	
P1	c.T127C (Homozygous)	p.W43R	Y	Y	Speech delay, triangular bird-like face, short philtrum	(Shaheen, et al., 2014)
P2	c.T127C (Homozygous)	p.W43R	Y	Y	NR	(Murray, et al., 2015)
P3	c.C481T c.C673T	p.R161X p.R225X	Y	Y	Gastrostomy, ectopic kidney, small bilateral kidneys, chronic lung disease	(Murray, et al., 2015)
P4-1#	c.C25del c.C823T	p.H9Tfs* 8 p.R275X	Y	Y	NR	(Murray, et al., 2015)
P4-2#	c.C25del c.C823T	p.H9Tfs* 8 p.R275X	Y	Y	NR	(Murray, et al., 2015)
P5	c.C25del c.C823T	p.H9Tfs* 8 p.R275X	Y	Y	Unilateral renal agenesis, cryptorchidism	(Murray, et al., 2015)
P6	c.C25del c.G-10-1T	p.H9Tfs* 8 splicing defect	Y	Y	Eczema	(Murray, et al., 2015)
P7-1#	c.C673T (Homozygous)	p.R225X	NR	Y	Adult-onset cardiomyopathy, neurological disorders, short limbs, pes avus, bilateral	(Bee, et al., 2015)

					cryptorchidism, hypotelorism	
P7-2#	c.C673T (Homozygous)	p.R225X	NR	Y	Adult-onset cardiomyopathy, neurological disorders, short limbs, pes avus, bilateral cryptorchidism, hypotelorism	(Bee, et al., 2015)
P8-1#	c.T246G, c.247_315 del (Homozygous)	p.D83E, p.V83_S 105del	Y	Y	Primary gonadal failure, type 2 diabetes, dyslipidemia, acanthosis, clinodactyly, cataracts, multinodular goiter	(de Bruin, et al., 2015)
P8-2#	c.T246G, c.247_315 del (Homozygous)	p.83del2 3, p.V83_S 105del	Y	Y	Primary gonadal failure, type 2 diabetes, dyslipidemia, acanthosis, clinodactyly, anemia, gastrointestinal stromal tumor (jejunum)	(de Bruin, et al., 2015)
P9-1#	c.G482A (Homozygous)	p.R161Q	Y	Y	Mild intellectual disability, facial dysmorphism	(Rosin, et al., 2015)
P9-2#	c.G482A (Homozygous)	p.R161Q	Y	Y	Mild intellectual disability, facial Dysmorphism	(Rosin, et al., 2015)
P9-3#	c.G482A (Homozygous)	p.R161Q	Y	Y	Mild intellectual disability, facial dysmorphism	(Rosin, et al., 2015)

P10	c.C25del c.C823T	p.His9Thr fs*8 p.R275X	Y	Y	Facial dysmorphism	(Rosin, et al., 2015)
P11	c.C673T c.G760del	p.R225X p.D254 Mfs*68	Y	Y	Progressive ataxia, hyperopia, diabetes mellitus, hypothyroidism, thalamic glioma, moderate hearing loss, slurred speech	(Guo, et al., 2015)

#: siblings. *Growth hormone treated.

Abbreviations: F, female; M, male; Y, yes; N, no; NR, not reported; y, year; m, month; SD, standard deviation; OFC, occipitofrontal circumference.

Successful mutagenesis was confirmed by nucleotide blast program comparing the nucleotide sequence to the original nucleotide sequence. The forward and reverse sequences of the mutations associated to development are found in Appendix 2. Then, constructs of wild-type XRCC4 and mutated XRCC4 were transfected into M10 or U2OS cells via Neon Transfection or Lipofection, respectively.

3.2 Protein Expression Level

Six XRCC4 mutations associated to development were successfully established which are point, deletion or frameshift mutations of XRCC4. As shown in Figure 9, the difference in XRCC4 protein's molecular weight between wild-type XRCC4 and the XRCC4 mutations are analyzed with gel electrophoresis and western blotting using anti-XRCC4, anti-FLAG antibodies and GAPDH as loading control. Filled triangles are bands for Wild-type XRCC4, W43R, R161Q, and D254Mfs*68, open triangles are bands for V83_S105del and R275X (upper), filled diamonds are bands for R275X

(lower) and open diamonds are bands for R225X. The stars in anti-FLAG blot indicate cross-reactive bands,

Results using anti-XRCC4 and anti-FLAG antibodies were mostly consistent, except for R225X and D254Mfs*68, which were not detected by anti-XRCC4. V83_S105del, R225X and D254Mfs*68 was expressed at a similar level to wild-type XRCC4 and W43R, R161Q and R275X were expressed at even higher level than wild-type XRCC4 (Figure 2). While the mobilities of W43R, R161Q, and D254Mfs*68 were like that of wild-type, V83_S105del, R225X, and R275X exhibited higher mobilities as expected from their molecular masses. R275X showed two bands of 50-55 kDa and 40-45 kDa in apparent molecular masses, respectively, the latter being more intense than the former. The upper band exhibited similar mobility to V83_S105del and appeared considerably larger than the expected size of R275X. Since the difference in the molecular mass of R275X and XRCC4(1-265) is 1.1kDa, the lower band would be more likely to be R275X. The identity of the upper band in R275X is currently unclear.

Since XRCC4 was shown to be required for the stability of LIG4 [13], the expression of LIG4 in these transfectants was also examined (Figure 9). The expression of LIG4 in the mutant XRCC4 transfectants was comparable to that in the wild-type XRCC4 transfectant, although it was substantially reduced in the control vector transfectant.

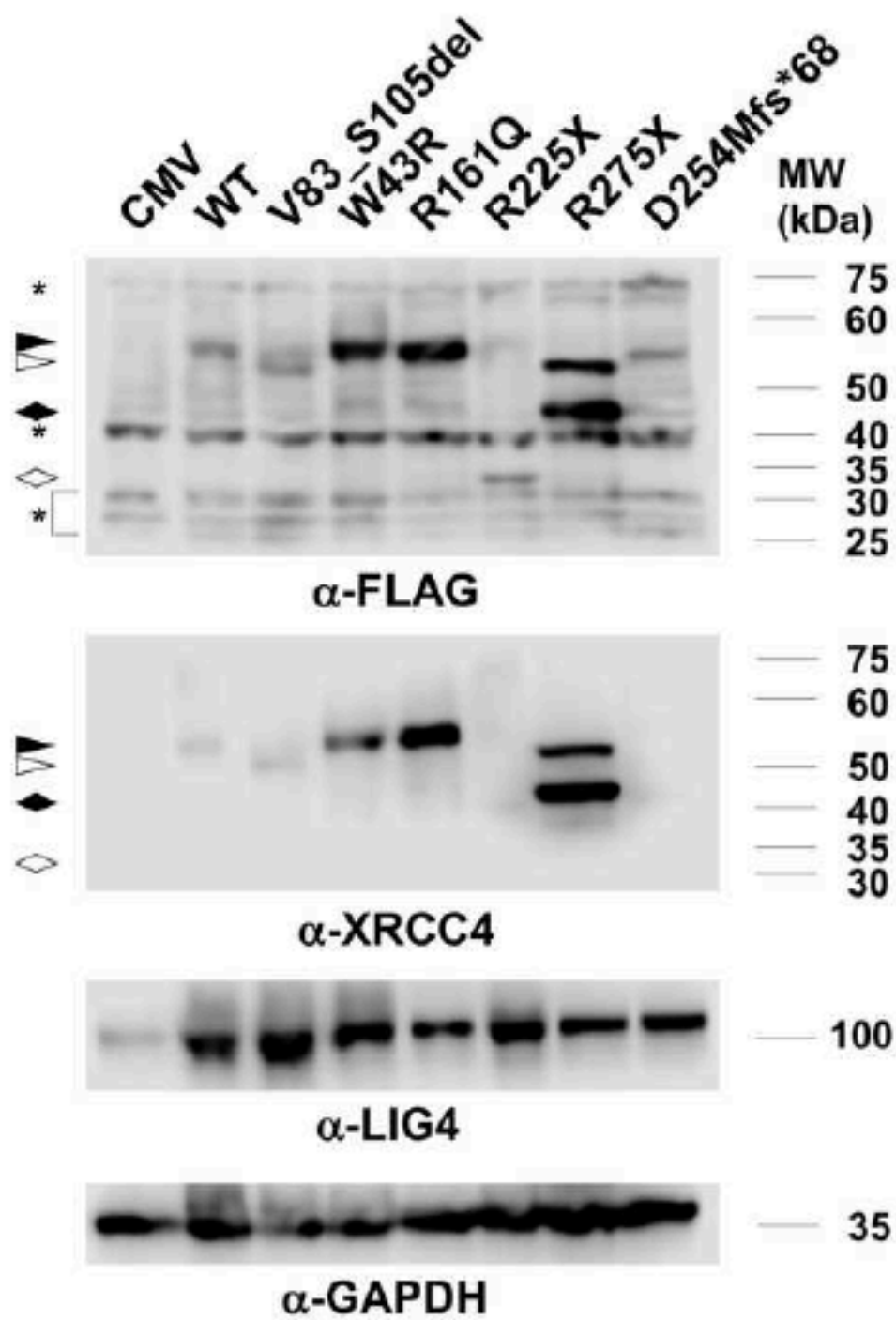


Figure 9. Expression levels of XRCC4 in M10-transfectants with wild-type and disease-associated mutants of XRCC4.

3.3. Nuclear Localization

To evaluate the ability of the XRCC4 mutations associated to development to localize to the nucleus where XRCC4 function is said to mostly located, cDNA for GFP-XRCC4 were generated and transiently expressed in U2OS cells. Live cell imaging of transfected U2OS cells reveal that XRCC4-WT localized to the nucleus, as well as mutated cells V83S-105del, W43R, R161Q and A247S. However, R225X, R275X and D254Mfs*68 did not localize to the nucleus, but instead localized in the cytoplasm (Figure 10). It can also be observed that the D254Mfs*68 showed punctated localization in the cytoplasm which is distinct from R225x and R275x.

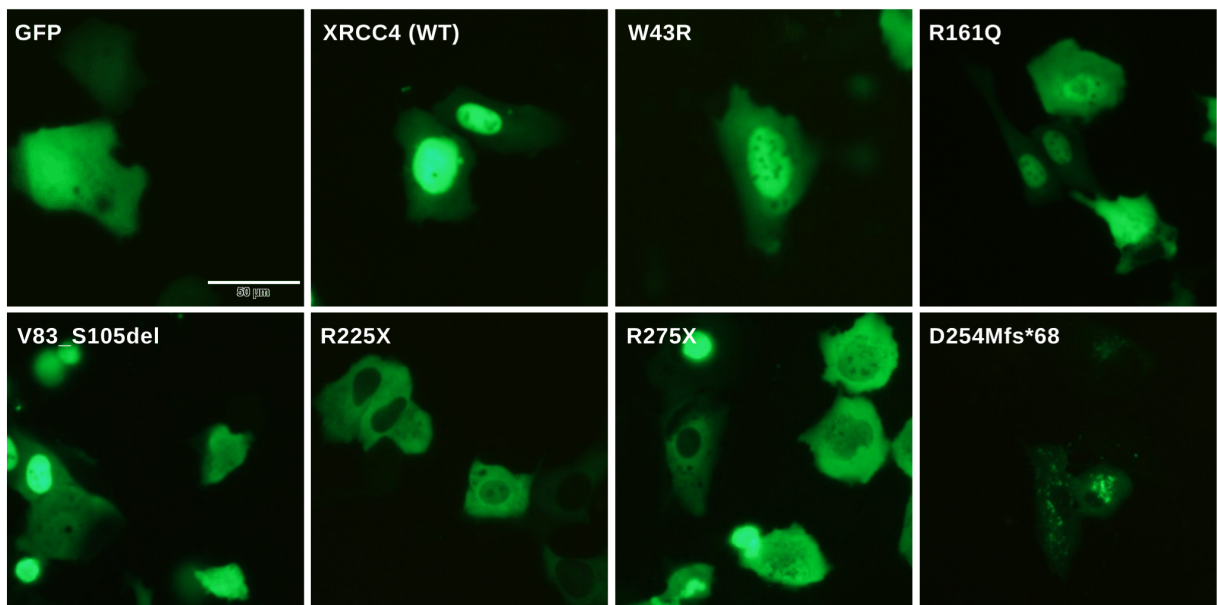
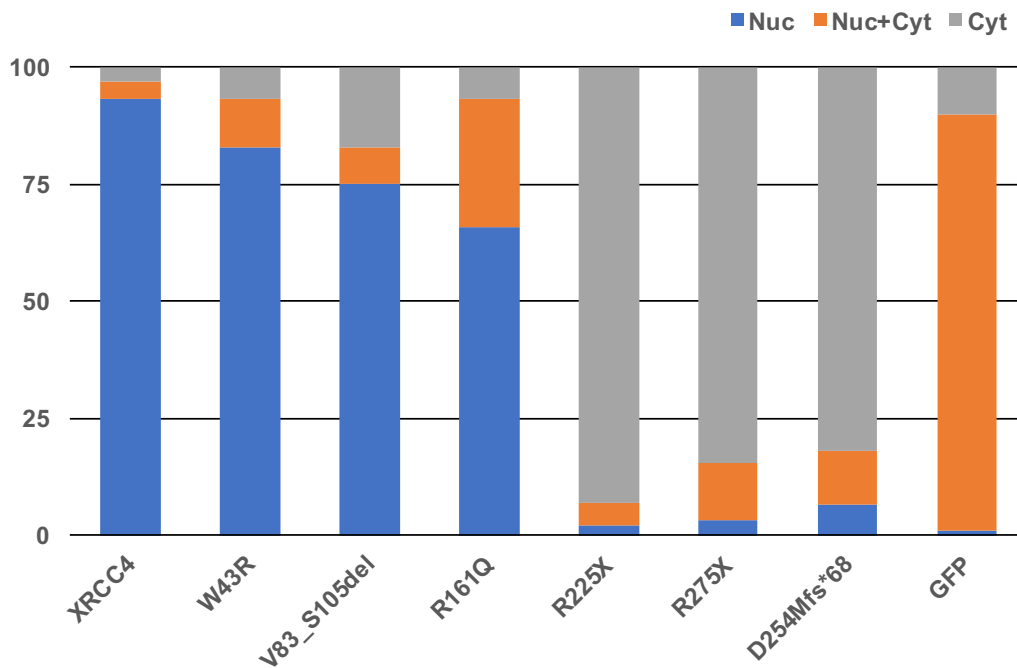


Figure 10. Localization of XRCC4 Mutations Associated to Development



**(Cells showing nuclear distribution (Nuc), nuclear plus cytoplasmic distribution (Nuc+Cyt) and cytoplasmic distribution (Cyt) were counted. Total number of counted cells was 100-128 for each transfectant.)*

Figure 11. Quantification of Subcellular localization of wild-type and disease-associated mutants of XRCC4 tagged with GFP

To confirm that the subcellular localization is not due to the endogenous XRCC4 present in the cell, knockdown of endogenous XRCC4 was done by SIRNA silencing. To knockdown endogenous XRCC4, small interfering RNA (siRNA targeting 3'-untranslated regions (UTR) was transfected 24 hours prior to plasmid transfection. The results shown in Figure 12 shows a consistent localization with V83-S105del, W43R and R161Q being localized in the nucleus and R225X, R275X and D254Mfs*68 localizing in the cytoplasm.

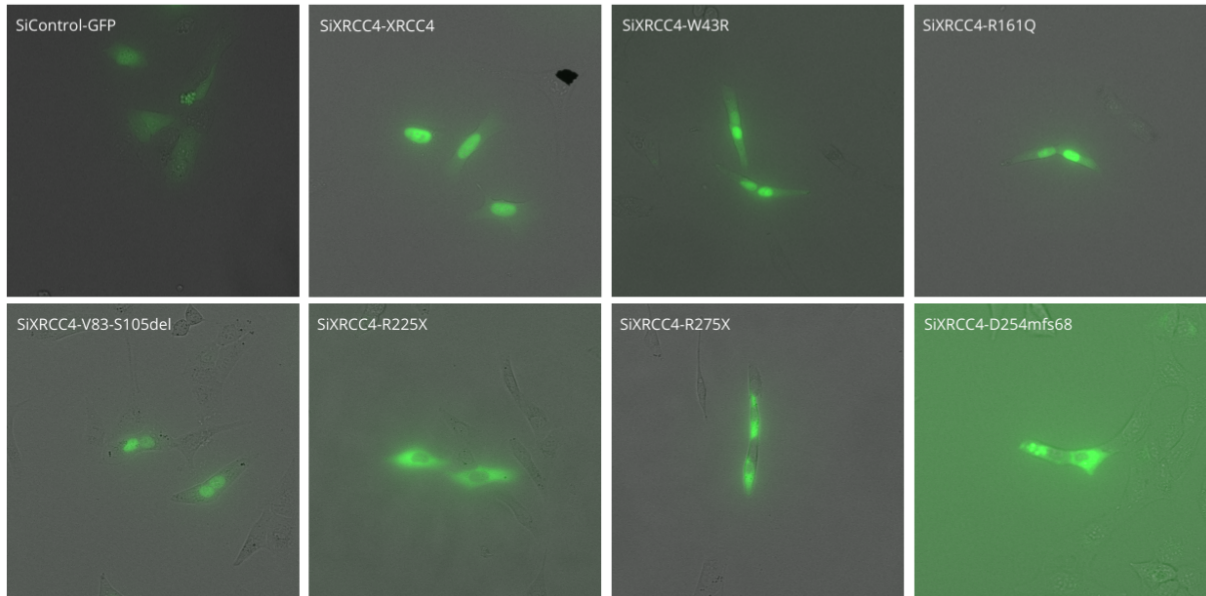


Figure 12. Localization of XRCC4 mutations Associated to Development without Endogenous XRCC4

3.4 Radiosensitivity

The radiosensitivity of XRCC4 mutants associated to development was assessed using colony formation assay after radiation exposure to γ -ray irradiation with irradiation doses of 2 and 4 Gray using Cobalt irradiation source (Figure 13). Statistical significance of difference between the mutations and wild-type XRCC4 was analyzed by two-way factorial analysis of variance. The mutation V83S-105del showed the highest radiosensitivity ($p=2.1 \times 10^{-8}$ with XRCC4). V83S-105del has long amino acid deletion near the sequence with association for XLF which may have caused most prominent change on its radiosensitivity. This mutation has nearly the same cell survival effect as the negative control CMV, in both radiation doses 2 Gy and 4 Gy and statistical significance test show no significant difference to control CMV ($p=0.42$). It may also be observed that D254Mfs*68 mutation also has showed substantially increased radiosensitivity compared to wild-type XRCC4 as shown by its less cell surviving fraction than radioresistant XRCC4 after irradiation at 2 Gy and 4 Gy with even more notable change at higher irradiation dose 4 Gy. ($p=5.6 \times 10^{-4}$), These results reveal partial function of D254Mfs*68 even if its protein was low, As compared with V83S-105del and D254Mfs*68, W43R, R161Q, R225x, and R275x have shown lesser difference in cell survival rate as the radioresistant XRCC4 although is still statistically significant (W43R $p=0.042$; R161Q $p=0.018$; R225X $p=0.018$ and R275X $p=0.014$ in comparison with XRCC4) indicating only partial loss of function. With increase in irradiation, the mutations tend to be more radiosensitive as what can be observed in the effect of surviving fraction at 4 Gy.

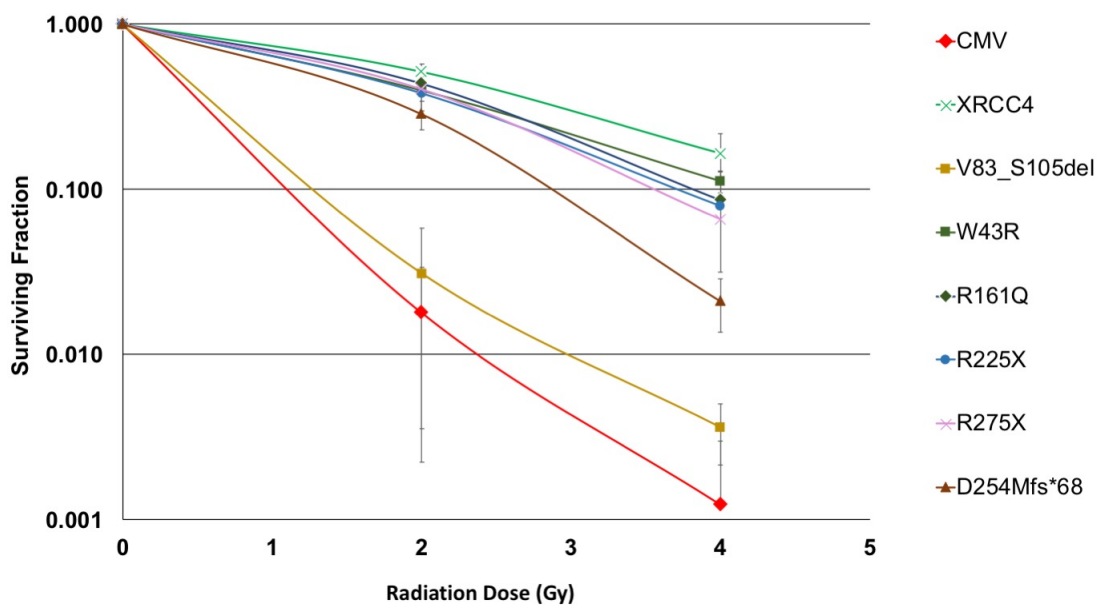


Figure 13. Radiosensitivity of XRCC4 mutation associated to Development

3.5 Structural Differences of XRCC4 Point Mutations Associated to Development

Table 5 is a summary of the changes that have occurred to the structure of XRCC4 after two point mutations, W43R and R161Q. As shown in Table 5, the stability after point mutation is computed using delta delta G which gives the value for change in Gibbs free energy after point mutation using its 3D structure and Normal mode Analysis. W43R was computed to be destabilizing the structure of XRCC4 possible due to the change in molecular weight and polarity from the change in side change from Tryptophan to Arginine. On the other hand, R161Q mutation cause a change of Arginine to Glutamine which is a neutral amino acid with lesser molecular weight that Arginine. The mutation was computed to cause a slight decrease in stability of the XRCC4 structure and an increase in the stability with the structure when bound to Ligase IV.

Table 5. Changes in the Structure of XRCC4 Point Mutations Associated to Development

Mutation	Amino acid	Change in Polarity	Change in charge	Molecular weight (g/mol)	Classification	$\Delta\Delta G^1$ (kcal/mole)	
						XRCC4	XRCC4 with BRCT ² of Ligase IV
W43R	Tryptophan-Arginine	Non-polar to polar	Neutral to positive	Tryptophan: 204.23 Arginine: 174.20	Tryptophan: Aromatic Arginine: Basic	-0.688 (destabilizing)	-0.887 (destabilizing)
R161Q	Arginine-Glutamine	No change (Polar)	Positive to neutral	Arginine: 174.20 Glutamine: 146.15	Arginine: Basic Glutamine: Neutral	-0.009 (destabilizing)	0.239 (stabilizing)

¹ $\Delta\Delta G$ – protein stability change upon mutation.

²BRCT – BRCA1 carboxyl terminus domains; DNA ligase IV associates with XRCC4 via its tandem BRCT domains

3.6 Discussion

In 2015, several patients reported with diseases associated to growth and development manifesting from their early years were reported to bear mutations on XRCC4 gene as shown in whole exome sequencing of their gene. To understand the changes that these mutations on the XRCC4 function in DNA repair, XRCC4 mutations were generated in the same background and functional characteristics of these mutations were investigated. Results showed varying degree of protein expression, subcellular localization and increased radiosensitivity of XRCC4 mutants associated to development compared to wild-type XRCC4.

V83-S105del showed highest radiosensitivity, which is not significantly different to the control CMV vector transfectant. V83-S105del was expressed at similar level to wild-type XRCC4 in its protein expression although lower than W43R, R161Q, R225X and R275X, and could be localized to the nucleus. Additionally, LIG4 expression in V83_S105del was comparable to that in wild-type XRCC4 transfectant. However, this mutant is presumed to be defective in interaction with XLF, which requires XRCC4 amino acids 59-106 (de Bruin, et al., 2015).

D254Mfs*68 transfectant showed the second highest radiosensitivity. The protein expression of D254Mfs*68 with XRCC4 antibody was undetectable in XRCC4 antibody and low with FLAG antibody. The LIG4 expression in the D254Mfs*68 transfectant was comparable to the wild-type XRCC4 transfectant, but the D254Mfs*68 transfectant was more radiosensitive than the wild-type XRCC4 transfectant. This result indicated that D254Mfs*68 retained partial function, although protein expression was low. DSB repair defects of D254Mfs*68 mutant might be mainly due to low abundance. Additionally, punctuated cytoplasmic localization of D254Mfs*68 was observed. Guo et al. also reported that XRCC4 proteins, i.e., R225X and D254Mfs*68, distributed in the cytoplasm as well as in the nucleus

of the fibroblast (Guo, et al., 2015). Considering this, the attachment of sequences due to frameshift in D254Mfs*68 might have caused a peculiar distribution in the nucleus and in the cytoplasm causing a change in XRCC4 function and stability.

R225X was expressed at a similar level to wild-type XRCC4; and W43R, R275X and R161Q were expressed at higher levels than wild-type XRCC4 in M10-transfectants. They could correct the radiosensitivity of M10 to the extent close to wild-type XRCC4. LIG4 was expressed at a comparable level in the transfectants of these mutants and the wild-type XRCC4 transfectant. These results indicated that these mutants were mostly functional when expressed at sufficient level and, therefore, XRCC4 defects in patients might be primarily due to low abundance of the proteins. Nonetheless, the radiosensitivity of the transfectants of these mutants was slightly but significantly higher than that of wild-type XRCC4 transfectant, suggesting that these mutants were not fully functional.

W43R is highly conserved among XRCC4 and in XLF and PAXX in wide range of eukaryotic species, suggesting its role in maintaining the structure of globular head domain of XRCC4 (Ochi, et al., 2012) (Xing, et al., 2015). Another study which reports on a close mutation to position 43 is a substitution mutation at position 53 which reports that this substitution could fully restore normal radio-sensitivity to M10 cells (Ropars, et al., 2011). These reports may support the results obtained with the radio-sensitivity of the W43R mutation with a slightly but significant decrease as compared to wild-type XRCC4 when protein expression has higher level of than that of wild-type XRCC4..

Bee et al. reported that XRCC4 protein expression was undetectable in patient with homozygous R225X mutation. Profound decrease of XRCC4 mRNA in these patients' fibroblasts suggested the involvement of nonsense-mediated decay due to longer C-terminal untranslated region than wild-type XRCC4 mRNA (Murray, et al., 2015). In this study, R225X mutant was expressed higher than wild-type XRCC4 and restored the radiosensitivity to a

similar extent to wild-type XRCC4. These results indicate the DSB repair defect in patient with R225X mutation might be mainly due to low abundance of protein due to the long deletion. R275X mutant was expressed at a higher level than XRCC4 and restored the radiosensitivity with a slight but significant to XRCC4. The difference in subcellular localization of R225x and R275x mutation to cytoplasm rather than nucleus, may have caused the slight but statistically significant decrease in cell survival after irradiation compared to wild-type XRCC4 transfectant. These may suggest the importance of nuclear localization signal as the major mechanism that drives XRCC4 to the nucleus. On the other hand, it is possible that because the XRCC4 is associated with DNA Ligase IV which is a nuclear protein with its own nuclear localization signal, the DNA Ligase IV may possibly drive XRCC4 to the nucleus at least even partially, causing a psrtial functional XRCC4 during DNA repair.

In the present study, R161Q expressed at higher level than wild-type XRCC4 and restored its radioresistance to an extent close to wild-type XRCC4 though statistically less than XRCC4, indicating that DSB repair defects in patients harboring this mutation might be attributable to low abundance. The slight but statistically significant increase in radiosensitivity of the R161Q transfectant as compared to wild-type XRCC4 transfectant in the current study might suggest possible effect of R161Q mutation on XRCC4 function. Arg161 is located close to the dimerization domain and region associated to Ligase IV interaction suggesting that the slight change in Arg161 may have caused a decrease in functionality as compared to XRCC4.

Several factors can account to the difference in protein expression of the different transfectants. DNA amount is equalized in this study, to ensure protein expression is equal. The CMV promoter for all constructs are the same, which allows high expression of mammalian cells. For some of the constructs, non-sense medicated decay may degrade the mRNA of the mutants. While point mutations are not subjected to non-sense mediated decay, premature stop codons such as truncation and frameshift mutations may be subjected to the

decay which may cause an effect to protein expression. For some mutants, low protein stability was also reported to the mRNA of patients. However, when protein expression is low, it is still possible to be functioning at low levels. Some mutants may be less abundant in expression than wild-type, but how much little is needed not to function is still unknown and may be studied in the future.

In previous research using a murine model, deficiency in XRCC4 results in a lethal embryonic phenotype with significant neuronal damage and extensive apoptosis, arrested lymphocyte development, as well as severe growth retardation and reduced fibroblast proliferation rates in vitro. These mice develop lymphomas and severe growth retardation, suggesting that XRCC4 deficiency leads to growth failure (Fukuchi, et al., 2015). The repair of DSBs is very crucial for the maintenance of genomic integrity. If DSBs are unrepaired, DSBs can induce apoptosis and give rise to increased cell death. XRCC4 serves as a modulator in the NHEJ pathway of DSB repair in mammals which is very significant for DNA repair and genomic instability.

Disease-associated mutations are then correlated with sensitivity or resistance to radiation. therapeutic agents, One of the patients with V83_S105del mutation was reported to have tumor complications (Table 3, Table 4, p8-2#). Since the results of radiosensitivity in this study show that V83S_105del was very radiosensitive, the proper choice of radiation and therapy should be assessed in treating the cancer complication. According to the report, however (de Bruin, et al., 2015), the patient did not have a history of acute radiation exposure or an increased cumulative radiation dose through repeated medical imaging before diagnosis of the tumor, but was on chemotherapy before her demise at age 36. Disease-associated mutations may also increase the risk of cancer, so screening, detection and monitoring of complications may also be considered when mutations in DNA repair such as XRCC4 are found out.

In summary, in this chapter, XRCC4 mutations associated with developmental diseases were successfully generated and analyzed in terms of its functional characteristics on the same background. The deletion mutation V83-S105del showed highest radiosensitivity which may have affected its XLF interaction. The frameshift mutation D254Mfs*68 also showed significantly higher radiosensitivity as compared to other mutations which may be caused by peculiar frameshift, localization and low protein abundance. For other mutations, substitution mutations W43R and R161Q, and deletion mutations R225X and R275X showed slight but significant increase in radiosensitivity with protein expression similar to XRCC4 or even at higher level than XRCC4. These results show that the defects of XRCC4 in disease patients might be due to insufficiency in protein quantity and impaired functionality.

Although immunodeficiency was not seen in many patients with XRCC4 mutations, it may be possible that the overall DNA changes in DNA repair function causes significant changes which is manifesting in e.g. development, therefore causing microcephaly and growth defects, as well as other complications. These findings reveal the significance of certain locations in the structure of XRCC4 as well as in its function in DNA repair through the NHEJ pathway. These reiterate the role of the integrity of XRCC4 to normal DNA DSB repair and in normal development and in the non-occurrence of diseases such as those related to development.

Chapter 5. Conclusion

Chapter 5

Conclusion

In this study, six XRCC4 mutations associated with development, and one XRCC4 mutation associated to cancer risk was successfully generated and introduced to cells lacking XRCC4 in order to delve deeper to the function of the structure, and the significance of the integrity of XRCC4 in the DNA repair, as well as its role in the non-progression and risk of diseases. The functionality of the XRCC4 mutations associated to development was studied in terms of protein expression level, subcellular localization and ability of the cells to survive after radiation exposure as shown by their radiosensitivity. On the other hand, the mutation associated to cancer was studied in terms of subcellular localization, DNA DSB repair by gamma H2Ax fluorescence as well as radiosensitivity.

As a summary, the deletion mutation V83-S105del showed highest radiosensitivity in all XRCC4 mutations associated to development in which the radiosensitivity was close to control vector transfectant. This result shows the significance of the location of XLF interaction in the N-terminal region in XRCC4 function in DNA repair. On the other hand, for the frameshift mutation D254Mfs*68, its higher radiosensitivity as compared to other mutations may have been caused by its subcellular localization and low protein abundance caused by the aberrant sequence formed after the frameshift. For mutations W43R and R161Q, and deletion mutations R225X and R275X, these mutations showed slight but significant increase in radiosensitivity compared to the wild-type XRCC4 even if the proteins are expressed at about equal or even higher level than wild-type XRCC4, which may show partial function of XRCC4 being retained in these mutations but still causing an effect in its cell survival. When expressed in human osteosarcoma cells, R225X, R275X and D254Mfs*68 localized to the cytoplasm, whereas other mutants localized to the nucleus. These findings reveal that the defects of

XRCC4 in patients harboring these mutations may be from insufficiency in protein quantity and impaired functionality. The present study shows the importance of XRCC4's DSB repair function in normal development, the significance of certain locations in the structure of XRCC4 as well as significance of a normal functioning DNA repair system for proper development and non-progression of diseases.

For mutation associated to cancer, the mutation A247S caused a change in subcellular localization of XRCC4 in human osteosarcoma cells. The increase in cytoplasmic localization and cells without nuclear localization as compared to wild-type XRCC4 shows the significance of conserved nuclear localization signal of XRCC4, as well as several phosphorylation sites and ubiquitylation site near this polymorphism. The change in chromatin recruitment, the change in recruitment to DNA damage after micro-irradiation, the radiosensitivity, as well as the significant increase in gamma H2Ax foci which is an indicator of DSB repair, indicates that A247S polymorphism has deficiencies in DNA DSB repair through NHEJ which may lead to improper gene function leading to tumorigenesis and cancer development.

In conclusion, XRCC4 has shown to be an important NHEJ protein to maintain genomic stability, and for protection and inhibition of diseases such as those related to development and cancer. XRCC4 mutations may have likely resulted in overall reduction in efficiency of NHEJ repair explaining dwarfism and microcephaly, and greater cancer risks. This stresses the role that DNA repair mechanisms play in disease development. XRCC4 mutations may cause severe effects as well as increase the risk of developmental defects and progression of cancer. When mutations to XRCC4 are found out and assessed, early detection, monitoring, prevention of diseases may be possible.

References

- Ahnesorg, P., Smith, P., & Jackson, S. P. (2006, January 27). XLF interacts with the XRCC4-DNA ligase IV complex to promote DNA nonhomologous end-joining. *Cell*, 124(2), 301-313.
- Andres, S. N., Vergnes, A., Ristic, D., Wyman, C., Modesti, M., & Junop, M. (2012). A human XRCC4-XLF complex bridges DNA. *Nucleic Acids Res.*, 40(4), 1868-78.
- Balashov, Viacheslavovich, V., & Pontecorvo, G. B. (1997). *Interaction of Particles and Radiation with Matter*. Berlin: Springer.
- Bee, L., Nasca, A., Zanolini, A., Cendron, F., d'Adamo, P., Costa, R., . . . Zeviani, M. (2015). A nonsense mutation of human XRCC4 is associated with adult-onset progressive encephalomyopathy. *EMBO Mol Med.*, 7(7), 918-29.
- Berg, E., Christensen, M. O., Rosaa, I. D., Wannagata, E., Jänicke, R. U., Rösner, L. M., . . . Mielke, C. (2011). XRCC4 controls nuclear import and distribution of Ligase IV and exchanges faster at damaged DNA in complex with Ligase IV. *DNA Repair (Amst.)*, 10(12), 1232-1242.
- Bryans, M., Valenzano, M. C., & Stamato, T. D. (1999, January 26). Absence of DNA ligase IV protein in XR-1 cells: evidence for stabilization by XRCC4. *Mutat Res.*, 433(1), 53-8.
- Buck, D., Malivert, L., de Chasseval, R., Barraud, A., Fondaneche, M.-C., Sanal, O., . . . Revy, P. (2006, January 27). Cernunnos, a novel nonhomologous end-joining factor, is mutated in human immunodeficiency with microcephaly. *Cell*, 124(2), 287-99.
- Chang, H. H., Pannunzio, N. R., Adachi, N., & Lieber, M. R. (2017, August). Non-homologous DNA end joining and alternative pathways to double-strand break repair. *Nat Rev Mol Cell Biol.*, 18(8), 495-506. doi:10.1038/nrm.2017.48
- Chen, X. (2013). Mechanism of Homologous recombination and implications for aging-related deletions in mitochondrial DNA. (476-96, Ed.) *Microbiol Mol Biol Rev*, 77(3).
- Cherry, A. L., Nott, T. J., Kelly, G., Rulten, S. L., Caldecott, K. W., & Smerdon, S. J. (2015). Versatility in phospho-dependent molecular recognition of the XRCC1 and XRCC4 DNA-damage scaffolds by aprataxin-family FHA domains. *DNA Repair (Amst.)*, 35, 116-25.

- Cifci, S., Yilmaz, M., Pehlivan, M., Sever, T., Okan, V., & Pehlivan, S. (2011, Nov). DNA repair genes polymorphisms in multiple myeloma: no association with XRCC1 (Arg399Gln) polymorphism, but the XRCC4 (VTNR in intron 3 and G-1394T) and XPD (Lys751Gln) polymorphisms is associated with the disease in Turkish patients. *Hematology*, 16(6), 361-7.
- Clements, P. M., Breslin, C., Deeks, E. D., Byrd, P. J., Ju, L., Bieganowski, P., . . . Caldecott, K. W. (2004). The ataxia-oculomotor apraxia 1 gene product has a role distinct for ATM and interacts with the DNA strand break repair proteins XRCC1 and XRCC4. *DNA Repair (Amst.)*, 3(11), 1493-502.
- Commission, C. N. (2012). *Introduction to Radiation*. Ottawa: Canadian Nuclear Safety Commission.
- Craxton, A., Somers, J., Munnur, D., Jukes-Jones, R., Cain, K., & Malewicz, M. (2015, June). XLS (c9orf142) is a new component of mammalian DNA double-stranded break repair. *Cell Death Differ*, 22(6), 890-7.
- Critchlow, S., Bowater, R., & Jackson, S. (1997). Mammalian DNA double-strand break repair protein XRCC4 interacts with DNA ligase IV. *Curr Biol.*, 7(8), 588-598.
- de Bruin, C., Mericq, V., Andrew, S. F., Duyvenvoorde, H. A., Verkaik, N. S., Losekoot, M., . . . Daubercorr, A. (2015). An XRCC4 splice mutation is associated with severe short stature, gonadal failure, and early-onset metabolic syndrome. *J Clin Endocrinol Metab*, 100(5), E789-98.
- Desouky, O., Ding, N., & Zhou, G. (2015). Targeted and non-targeted effects of ionizing radiation. *J Radiat Res Appl*, 8(2), 247-254.
- DiBiase, S. J., Zeng, Z. C., Chen, R., Hyslop, T., Curran, W., & Iliakis, G. (2000). DNA-dependent protein kinase stimulates an independently active, nonhomologous, end-joining apparatus. *Cancer Res.*, 60(5), 1245-53.
- Difilippantonio, M. J., Zhu, J., Che, H., Meffre, E., Nussenzweig, M. C., Max, E. E., . . . Nussenzweig, A. (2000). DNA repair protein Ku80 suppress chromosomal aberrations and malignant transformation. *Nature*, 404, 510-14.
- Dueva, R., & Iliakis, G. (2013, June). Alternative pathways of non-homologous end joining (NHEJ) in genomic instability and cancer. *Transl Cancer Res.*, 2(3), 163-77.
- Frank, K. M., Sekiguchi, J. M., Seidl, K. J., Swat, W., Rathbun, G. A., Cheng, H. L., . . . Alt, F. W. (1998, Nov 12). Late embryonic lethality and impaired V(D)J recombination in mice lacking DNA ligase IV. *Nature*, 396(6707), 173-7.

- Frank, K. M., Sharpless, N. E., Gao, Y., Sekiguchi, J. M., Ferguson, D. O., Zhu, C., . . . Alt, F. W. (2000). DNA ligase IV deficiency in mice leads to defective neurogenesis and embryonic lethality via the p53 pathway. *Mol Cell.*, 5(6), 993-1002.
- Fukuchi, M., Wanotayan, R., Liu, S., Imamichi, S., Sharma, M. K., & Matsumoto, Y. (2015). Lysine 271 but not lysine 210 of XRCC4 is required for the nuclear localization of XRCC4 and DNA ligase IV. *Biochem Biophys Res Commun.*, 461(4), 687-694.
- Gao, Y., Ferguson, D. O., Xie, W., Manis, J. P., Sekiguchi, J., Frank, K. M., . . . Alt, F. W. (2000). Interplay of p53 and DNA-repair protein XRCC4 in tumorigenesis genomic stability and development. *Nature*, 404, 879-900.
- Gao, Y., Sun, Y., Frank, K., Dikkes, P., Fujiwara, Y., Seidl, K., . . . Alt, F. (1998). A critical role for DNA end-joining proteins in both lymphogenesis and neurogenesis. *Cell*, 95(7), P891–902.
- Gauss, G. H., & Lieber, M. R. (1993, Jul). Unequal signal and coding joint formation in human V(D)J recombination. *Mol Cell Biol*, 13(7), 3900-6. doi:10.1128/mcb.19.7.3900
- Gavande, N. S., VanderVere-Carozza, P. S., Hinshaw, H. D., Jalal, S. I., Sears, C. R., Pawelc, K. S., & zak, J. J. (2016). DNA repair targeted therapy: The past or future of cancer treatment? *Pharmacol Ther.*, 160, 65-83.
- Grawunder, U., Wilm, M., Wu, X., Kulesza, P., Wilson, T., Mann, M., & Lieber, M. (1997). Activity of DNA ligase IV stimulated by complex formation with XRCC4 protein in mammalian cells. *Nature*, 388(6641), 492-95.
- Grawunder, U., Zimmer, D., Kulesza, P., & Lieber, M. R. (1998). Requirement for an interaction of XRCC4 with DNA Ligase IV for Wild-type V(D)J Recombination and DNA Double-strand Break Repair in Vivo. *J Biol Chem.*, 273(38), 24708-24714.
- Gu, Y., Sekiguchi, J., Gao, Y., Dikkes, P., Frank, K., Ferguson, D., . . . Alt, F. W. (2000). Defective embryonic neurogenesis in Ku-deficient but not DNA-dependent protein kinase catalytic subunit-deficient mice. *P Natl Acad Sci USA.*, 97(6), 2668-73.
- Guo, C., Nakazawa, Y., Woodbine, L., Bjorkman, A., Shimada, M., Fawcett, H., . . . Ogi, T. (2015). XRCC4 deficiency in human subjects causes a marked neurological phenotype but no overt immunodeficiency. *J Allergy Clin Immunol.*, 136(4), 1007-1017.
- Hall EJ, Giaccia AJ. *Cell Survival Curves. Radiobiology for the Radiologist.* 7th Ed. 2012, 35-53.
- Hammel, M., Yu, Y., Fang, S., Lees-Miller, S. P., & Tainer, J. A. (2010, Nov 10). XLF regulates filament architecture of the XRCC4: ligase IV complex. *Structure*, 18(11), 1431-1442.

- Han, W., & Yu, K. N. (2010). Ionizing radiation, DNA double strand break and mutation. In K. V. Urbano, *Advances in Genetics Research* (pp. 1-13). Hongkong: Nova Science Publishers, Inc.
- He, M., Hu, X., Chen, L., Cao, A.-Y., Yu, K.-D., Shi, T.-Y., . . . Shao, Z.-M. (2014). A recessive variant of XRCC4 predisposes to non-BRCA1/2 breast cancer in chinese women and impairs the DNA damage response via dysregulated nuclear localization. *Oncotarget.*, 5(23), 12218-32.
- Hoeijmakers, J. H. (2001). Genome maintenance mechanisms for preventing cancer. *Nature*, 411, 366-374.
- Iles, N., Rulten, S., El-Khamisy, S. F., & Caldecott, K. W. (2007). APLF (C2orf13) is a novel human protein involved in the cellular response to chromosomal DNA strand breaks. *Mol Cell Biol.*, 27(10), 3793-803.
- Imamichi, S., Sharma, M. K., Kamdar, R. P., Fukuchi, M., & Matsumoto, Y. (2014). Ionizing radiation-induced XRCC4 phosphorylation is mediated through ATM in addition to DNA-PK. *Proc Jpn Acad Ser B-Phys Biol Sci.*, 90(9), 365-372.
- Junop, M. S., Modesti, M., Guarné, A., Ghirlando, R., Gellert, M., & Yang, W. (2000). Crystal structure of the XRCC4 DNA repair protein and implications for end joining. *EMBO J*, 19(22), 5962-70.
- Kamdar, R., & Matsumoto, Y. (2010). Radiation-induced XRCC4 association with chromatin DNA analyzed by biochemical fractionation. *J Radiat Res.*, 51(3), 303-313.
- Kanno, S.-i., Kuzuoka, H., Sasao, S., Hong, Z., Lan, L., Nakajima, S., & Akira, Y. (2007). A novel human AP endonuclease with conserved zinc-finger-like motifs involved in DNA strand break responses. *EMBO J*, 26(8), 2094-103.
- Kelsey, C.A., Heintz, P.H., Sandoval D.H., Chambers, G.D., Adolphi N.L., Paffett K.S. (2014). *Radiobiology of Medical Imaging*. 1-315.
- Koch, C., Agyei, R., Galicia, S., Metalnikov, P., O'Donnel, P., Starostine, A., . . . Durocher, D. (2004). Xrcc4 physically links DNA end processing by polynucleotide kinase to DNA ligation by DNA ligase IV. *EMBO J.*, 23(19), 3874-85.
- Leber, R., Wise, T. W., Mizuta, R., & Meek, K. (1998). The XRCC4 gene product is a target for and interacts with the DNA-dependent protein kinase. *J Biol Chem.*, 273(3), 1794-801.
- Lee, K. J., Huang, J., Takeda, Y., & Dynan, W. S. (2000). DNA ligase IV and XRCC4 form a stable mixed tetramer that functions synergistically with other repair factors in a cell-free end-joining system. *J Biol Chem.*, 275, 34787-96.

- Lee, K., Jovanovic, M., Udayakumar, D., Bladen, C., & Dynan, W. (2004). Identification of DNA-PKcs phosphorylation sites in XRCC4 and effects of mutations at these sites on DNA end joining in a cell-free system. *DNA Repair (Amst.)*, 3(3), 267-76.
- Li, W., Bai, X., Li, J., Zhao, Y., Liu, J., Zhao, H., . . . Xu, D. (2019, Sep 23). The nucleoskeleton protein IFF01 immobilizes broken DNA and suppresses chromosome translocation during tumorigenesis. *Nat Cell Biol*, 21, 1273-1285.
- Li, Z., Otevrel, T., & Gao, Y. (1995). The XRCC4 gene encodes a novel protein involved in DNA double-strand break repair and V(D)J recombination. *Cell*, 83(7), 1079-1089.
- Lieber, M. R. (2010). The mechanism of double-strand DNA break repair by the nonhomologous DNA end joining pathway. *Annu Rev Biochem.*, 79, 181-211.
- Lin, Z.-H., Chen, J.-C., Wang, Y.-S., Huang, T.-J., Wang, J., & Long, X.-D. (2013, Dec 27). DNA repair gene XRCC4 codon 27 polymorphism modified diffusely infiltrating astrocytoma risk and prognosis. *Int J Mol Sci*, 15(1), 250-60. doi:10.3390/ijms15010250
- Lodish, H., Berk, A., Zipursky, S. L., Matsudaira, P., Baltimore, D., & Darnell, J. (2000). *Molecular Cell Biology* (4th ed.). New York: W. H. Freeman.
- Lomax, M. E., Folkes, L. K., & O'Neill, P. (2013). Biological consequences of radiation-induced DNA damage: relevance to radiotherapy. *Clin Oncol (R Coll Radiol.)*, 25(10), 578-85.
- Long, X.-D., Yao, J.-G., Zeng, Z., Ma, Y., Huang, X.-Y., Wei, Z.-H., . . . Xia, Q. (2013, Jul). Polymorphisms in the coding region of X-ray repair complementing group 4 and aflatoxin B1-related hepatocellular carcinoma. *Hepatology*, 58(1), 171-81. doi:10.1002/hep.26311
- Macrae, C. J., McCulloch, R. D., Ylanko, J., Durocher, D., & Koch, C. (2008). APLF (C2orf13) facilitates nonhomologous end-joining and undergoes ATM-dependent hyperphosphorylation following ionizing. *DNA Repair (Amst.)*, 7(2), 292-302.
- Mahaney, B. L., Hammel, M., Meek, K., Tainer, J. A., & Lees-Miller, S. P. (2013). XRCC4 and XLF form long helical protein filaments suitable for DNA end protection and alignment to facilitate DNA double strand break repair. *Biochem Cell Biol.*, 91(1), 31-41.
- Matsumoto, Y., Suzuki, N., Namba, N., Umeda, N., Ma, X., Morita, A., . . . Hosoi, Y. (2000). Cleavage and phosphorylation of XRCC4 protein induced by X-irradiation. *FEBS Lett.*, 478, 67-71.

- Matsumoto, Y., Suzuki, N., Sakai, K., Morimatsu, A., Hirano, K., & Murofushi, H. (1997, May 29). A possible mechanism for hyperthermic radiosensitization mediated through hyperthermic lability of Ku subunits in DNA-dependent protein kinase. *Biochem Biophys Res Comm*, 234(3), 568-72.
- Modesti, M., Hesse, J. E., & Gellert, M. (1999). DNA binding of Xrcc4 protein is associated with V(D)J recombination but not with stimulation of DNA ligase IV activity. *EMBO J*, 18(7), 2008-18.
- Moghani, A., Sharma, M., & Matsumoto, Y. (2018). In cellulo phosphorylation of DNA double-strand break repair protein XRCC4 on Ser260 by DNA-PK. *J Radiat Res.*, 59(6), 700-708.
- Mori, M., Itsukaichi, H., Nakamura, A., & Sato, K. (2001). Molecular characterization of ionizing radiation-hypersensitive mutant M10 cells. *Mutation Research*, 487: 85-92.
- Murray, J. E., van der Burg, M., IJspeert, H., Carroll, P., Wu, Q., Ochi, T., . . . Bicknell, L. S. (2015). Mutations in the NHEJ component XRCC4 cause primordial dwarfism. *Am J Hum Genet.*, 96(3), 412-424.
- Nishana, M., & Raghavan, S. C. (2012). Role of recombination activating genes in the generation of antigen receptor diversity and beyond. *Immunology*, 137(4), 271-281.
- Normanno, D., Négre, A., de Melo, A. J., Betzi, S., Meek, K., & Modesti, M. (2017). Mutational phospho-mimicry reveals a regulatory role for the XRCC4 and XLF C-terminal tails in modulating DNA bridging during classical non-homologous end joining. *Elife*, 6:e22900.
- Ochi, T., Blackford, A. N., Coates, J., Jhujh, S., Mehmood, S., Tamura, N., . . . Jackson, S. P. (2015, January 09). PAXX, a paralog of XRCC4 and XLF, interacts with Ku to promote DNA double-strand break repair. *Science*, 347(6218), 185-188. doi:10.1126/science.1261971
- Ochi, T., Quarantotti, V., Lin, H., Julliean, J., Silva, I. E., Boselli, F., . . . van Breugel, M. (2020, June 2). CCDC61/VFL3 is a paralog of SAS6 and promotes ciliary functions. *Structure*, 28(6), 674-689.
- Ochi, T., Wu, Q., Chirgadze, D. Y., Grossmann, J. G., Bolanos-Garcia, V. M., & Blundell, T. L. (2012). Structural insights into the role of domain flexibility in human DNA ligase IV. *Structure*, 20-20(7), 1212–1222.
- Okayasu, R., Suetomi, K., Yu, Y., Silver, A., Bedford, J. S., Cox, R., & Ullrich, R. L. (2000). A deficiency in DNA Repair and DNA-PKcs expression in the radiosensitive BALB/c mouse. *Cancer Res.*, 60(16), 4342–45.

- Pannunzio, N. R., Watanabe, G., & Lieber, M. R. (2008, July 6). Nonhomologous DNA end-joining for repair of DNA double-strand breaks. *J Biol Chem.*, 293(27), 10512-23. doi:10.1074/jbc.TM117.000374
- Rao, K. S. (Spring 1993). Genomic damage and its repair in young and aging brain. *Mol Neurobiol*, 7(1), 23-48. doi:10.1007/BF02780607
- Rask, J., Vercoutere, W., Krause, A., & Navarro, B. (2007). Module 2: Radiation Damage in Living Organism. In NASA, *Space Faring: The Radiation Challenge* (pp. 1-19). Alabama: NASA.
- Ropars, V., Drevet, P., Legrand, P., Bacconnais, S., Amram, J., Faure, G., . . . Charbonnier, J.-B. (2011, Aug 2). Structural characterization of filaments formed by human Xrcc4-Cernunnos/XLF complex involved in nonhomologous DNA end-joining. *Proc Natl Acad Sci USA.*, 108(31), 12663-8.
- Rosin, N., Elcioglu, N. H., Beleggia, F., Isgüven, P., Altmüller, J., Thiele, H., . . . Yigit, G. (2015). Mutations in XRCC4 cause primary microcephaly, short stature and increased genomic instability. *Hum Mol Genet.*, 24(13), 3708-3717.
- Rothkamm, K., & Löbrich, M. (2003, Apr 29). Evidence for a lack of DNA double-strand break repair in human cells exposed to very low x-ray doses. *Proc Natl Acad Sci USA*, 100(9), 5057-62.
- Roy, S., Andres, S. N., Vergnes, A., Neal, J. A., Xu, Y., Yu, Y., . . . Meek, K. (2012, Feb). XRCC4's interaction with XLF is required for coding (but not signal) end joining. *Nucleic Acids Res*, 40(4), 1684-94.
- Sato, K., & Hieda, N. (1979). Isolation and characterization of a mutant mouse lymphoma cell sensitive to methyl methanesulfonate and X rays. *Radiat Res.*, 78(1), 167-171.
- Schipler, A., & Iliakis, G. (2013). DNA double-strand-break complexity levels and their possible contributions to the probability for error-prone processing and repair pathway choice. *Nucleic Acids Res.*, 41(16), 7589–605.
- Shaheen, R., Faqeih, E., Ansari, S., Abdel-Salam, G., Al-Hassnan, Z. N., Al-Shidi, T., . . . Alkuraya, F. S. (2014). Genomic analysis of primordial dwarfism reveals novel disease genes. *Genome Res*, 2, 291-9.
- Sharma, M., Imamichi, S., Fukuchi, M., Samarth, R., Tomita, M., & Matsumoto, Y. (2016). In cellulo phosphorylation of XRCC4 Ser320 by DNA-PK induced by DNA damage. *J Radiat Res.*, 57(2), 115-120.

- Sheehan, K. M., & Lieber, M. R. (1933, Mar). V(D)J recombination: signal and coding joint resolution are uncouple and depend on parallel synapsis of the sites. *Mol Cell Biol.*, 13(3), 1363-70.
- Sibanda, B. L., Critchlow, S. E., Begun, J., Pei, X. Y., Jackson, S. P., Blundell, T. L., & Pellegrini, L. (2001). Crystal structure of an Xrcc4–DNA ligase IV complex. *Nat Struc Mol Biol.*, 8, 1015-19.
- Terawasa, M., Shinohara, A., & Shinohara, M. (2014, Aug 28). Canonical non-homologous end joining in mitosis induces genome instability and is suppressed by M-phase-specific phosphorylation of XRCC4. *PLoS Genet*, 10(8).
- Terzoudi, G. I., Singh, S., Pantelias, G. E., & Iliakis, G. (2000, October 1). Premature chromosome condensation reveals DNA-PK independent pathways of chromosome break repair. *Int J Oncol.*, 33(4), 871-879. doi:10.3892/ijo_00000075
- Tseng, H.-C., Tsai, M.-H., Chiu, C.-F., Wang, C.-H., Chang, N.-W., Huang, C.-Y., . . . Bau, D.-T. (2008, May-Jun). Association of XRCC4 codon 247 polymorphism with oral cancer susceptibility in Taiwan. *Anticancer Res*, 28(3A), 1687-91.
- Tsukada K, Shimada M, Imamura R. The FHA domain of PNKP is essential for its recruitment to DNA damage sites and maintenance of genome stability. *Mutat Res* 2020;822.
- Wang, C., & Lees-Miller, S. P. (2013). Detection and repair of ionizing radiation induced DNA double strand breaks: new developments in non-homologous end joining. *Int J Radiat Oncol Biol Phys.*, 86(3), 440-49.
- Wang, H., Perrault, A., Takeda, Y., Qin, W., Wang, H., & Iliakis, G. (2003, September 15). Biochemical evidence for Ku-independent backup pathways of NHEJ. *Nucleic Acids Res.*, 31(18), 5377-88. doi:10.1093/nar/gkg728
- Wanotayan, R., Fukuchi, M., Imamichi, S., Sharma, M., & Matsumoto, Y. (2015, Feb 20). Asparagine 326 in the extremely C-terminal region of the XRCC4 is essential for the cell survival after irradiation. *Biochem Biophys Res Commun.*, 457(4), 526-31.
- Ward, J. (1990). The yield of DNA double strand breaks produced intracellularly by ionizing radiation: a review. *Int J Radiat Biol*, 57(6), 1141-1150.
- Woodbine, L., Gennery, A. R., & Jeggo, P. A. (2014). The clinical impact of deficiency in DNA non-homologous end-joining. *DNA Repair (Amst).*, 16, 84-96.
- Xing, M., Yang, M., Huo, W., Feng, F., Wei, L., Jiang, W., . . . Xu, D. (2015, Feb 11). Interactome analysis identifies a new paralogue of XRCC4 in non-homologous end joining DNA re. *Nat Commun.*, 6(6233).

- Yu, H., Zhao, H., Wang, L.-E., Han, Y., Chen, W. V., Amos, C. I., . . . Wei, Q. (2011, Apr 3). An analysis of single nucleotide polymorphisms of 125 DNA repair genes in the Texas genome-wide association study of lung cancer with a replication for the XRCC4 SNPs. *DNA Repair (Amst.)*, 10(4), 398-407. doi:10.1016/j.dnarep.2011.01.005
- Yu, Y., Wang, W., Ding, Q. Y., Chen, D., Merkle, D., Schriemer, D., . . . Lees-Miller, S. (2003). DNA-PK phosphorylation sites in XRCC4 are not required for survival after radiation or for V(D)J recombination. *DNA Repair (Amst.)*, 2(11), 1239-52.
- Zhang, Q., Karnak, D., Tan, M., Lawrence, T. S., Morgan, M. A., & Sun, Y. (2016, Feb 4). FBXW7 facilitates nonhomologous end-joining via K63-linked polyubiquitylation of XRCC4. *Mol Cell*, 61(3), 419-433

Appendix

Appendix 1. Profile of Patients associated with XRCC4 Mutations

Patient	Gender	Country of origin	Consanguinity of parents	Change in nucleotide sequence	Change in amino acid sequence	Clinical features			Reference
						Microcephaly (OFC)	Short stature (Length/height)	Other features	
P1	F	Saudi Arabia	Y	c.T127C (Homozygous)	p.W43R	Y (4y:-8.3SD)	Y (4y:-7.1SD)	Speech delay, triangular bird-like face, short philtrum	(Shaheen, et al., 2014)
P2	M	Saudi Arabia	NR	c.T127C (Homozygous)	p.W43R	Y (Birth:-4.87SD; 3y1m:-8.3SD)	Y (Birth:-2.52SD; 3y1m:-4.7SD)	NR	(Murray, et al., 2015)
P3	M	Morocco	NR	c.C481T c.C673T	p.R161X p.R225X	Y (Birth:-4.57SD; 2y9m:-8.3SD)	Y (Birth:-6.32SD; 2y9m:-5.7SD)	Gastrostomy, ectopic kidney, small bilateral kidneys, chronic lung disease	(Murray, et al., 2015)
P4-1#	M	Italy	NR	c.C25del c.C823T	p.H9Tfs*8 p.R275X	Y (Birth:-2.9SD 8y4m:-5.6SD)	Y (Birth:-4.49SD 8y4m:-2.4SD)	NR	(Murray, et al., 2015)
P4-2#	M	Italy	NR	c.C25del c.C823T	p.H9Tfs*8 p.R275X	Y (Birth:-1.83SD; 4y:-8.0SD)	Y (Birth:-5.38SD; 4y:-4.5SD)	NR	(Murray, et al., 2015)
P5	M	France	NR	c.C25del c.C823T	p.H9Tfs*8 p.R275X	Y (Birth:-4.28SD; 9y:-5.8SD)	Y (Birth:-2.71SD; 9y, -1.8SD*)	Unilateral renal agenesis, cryptorchidism	(Murray, et al., 2015)

P6	M	United Kingdom	NR	c.C25del c.G-10-1T	p.H9Tfs*8 splicing defect	Y (Birth:-2.9SD; 5m, -8.9SD)	Short stature (Birth:-6.56SD; 5m, -7.2SD)	Eczema	(Murray , et al., 2015)
P7-1#	M	Italy	Y	c.C673T (Homozygous)	p.R225X	NR	Y	Adult-onset cardiomyopathy, neurological disorders, short limbs, pes avus, bilateral cryptorchidism, hypotelorism	(Bee, et al., 2015)
P7-2#	M	Italy	Y	c.C673T (Homozygous)	p.R225X	NR	Y	Adult-onset cardiomyopathy, neurological disorders, short limbs, pes avus, bilateral cryptorchidism, hypotelorism	(Bee, et al., 2015)
P8-1#	M	Chile	NR	c.T246G, c.247_315del (Homozygous)	p.D83E, p.V83- S105del	Y (39.9y:-3.3SD)	Y (Birth:-2.8SD; 39.9y:-6.8SD)	Primary gonadal failure, type 2 diabetes, dyslipidemia, acanthosis, clinodactyly, cataracts, multinodular goiter	(de Bruin, et al., 2015)
P8-2#	F	Chile	NR	c.T246G, c.247_315del (Homozygous)	p.83del23, p.V83- S105del	Y (36y:-2.9SD)	Y (Birth:-2.3SD; 36y:-4.0SD)	Primary gonadal failure, type 2 diabetes, dyslipidemia, acanthosis, clinodactyly, anemia, gastrointestinal stromal tumor (jejunum)	(de Bruin, et al., 2015)
P9-1#	M	Turkey	Y	c.G482A (Homozygous)	p.R161Q	Y (Birth:<-3SD; 14y:-7.5SD)	Y (Birth:-2 SD; 14y, -5SD)	Mild intellectual disability, facial Dysmorphism	(Rosin, et al., 2015)
P9-2#	M	Turkey	Y	c.G482A (Homozygous)	p.R161Q	Y (Birth:<-3SD; 10.5y:-6.5SD)	Y (Birth:NR; 10.5y:-5SD)	Mild intellectual disability, facial Dysmorphism	(Rosin, et al., 2015)
P9-3#	M	Turkey	Y	c.G482A (Homozygous)	p.R161Q	Y (Birth:<-3SD; 6m:-4.5SD)	Y (Birth:NR; 6m:-3SD)	Mild intellectual disability, facial Dysmorphism	(Rosin, et al., 2015)

P10	F	Switzerland	NR	c.C25del c.C823T	p.His9Thrfs *68 p.R275X	Y (Birth:-3.7SD; 14y10m:- 5.0SD)	Y (Birth:-2.8SD; 14y10m:- 2.6SD)	Facial dysmorphism	(Rosin, et al., 2015)
P11	F	United Kingdom	N	c.C673T c.G760del	p.R225X p.D254fs*6 8	Y	Y	Progressive ataxia, hyperopia, diabetes mellitus, hypothyroidism, thalamic glioma, moderate hearing loss, slurred speech	(Guo, et al., 2015)

#: siblings. *Growth hormone-treated.

Abbreviations: F, female; M, male; Y, yes; N, no; NR, not reported; y, year; m, month; SD, standard deviation; OFC, occipitofrontal circumference.

Appendix 2 - Sequence Check After Mutagenesis of XRCC4 Mutation Associated to Development

V83_S105DEL - FORWARD

Range 1: 5 to 503 [Graphics](#) ▼ Next Match ▲ Previous Match

Score	Expect	Identities	Gaps	Strand
917 bits(496)	0.0	498/499(99%)	0/499(0%)	Plus/Plus
Query 510	AGCTTTGGAGACTGATCTTTATAAGCGGTTTATTCTGGTGTGAATGAGAAGAAAACAAA	569		
Sbjct 5	AGCTTTGGAGACTGATCTTTATAAGCGGTTTATTCTGGTGTGAATGAGAAGAAAACAAA	64		
Query 570	AATCAGAAGTTTGCATAATAAATTTATAAATGCAGCTCAAGAACGAGAAAAGGACATCAA	629		
Sbjct 65	AATCAGAAGTTTGCATAATAAATTTATAAATGCAGCTCAAGAACGAGAAAAGGACATCAA	124		
Query 630	ACAAGAAGGGGAACTGCAATCTGTTCTGAAATGACTGCTGACCAGATCCAGTCTATGA	689		
Sbjct 125	ACAAGAAGGGGAACTGCAATCTGTTCTGAAATGACTGCTGACCAGATCCAGTCTATGA	184		
Query 690	TGAGAGTACTGATGAGGAAAGTGAACCCTGATCTCTCTGGGTTGGCTTCAGTCTGC	749		
Sbjct 185	TGAGAGTACTGATGAGGAAAGTGAACCCTGATCTCTCTGGGTTGGCTTCAGTCTGC	244		
Query 750	TGTAAGTAAAGATGATCCATTATTCAAGTCTTGATGTCACTGATATGCACCAAGTAG	809		
Sbjct 245	TGTAAGTAAAGATGATCCATTATTCAAGTCTTGATGTCACTGATATGCACCAAGTAG	304		
Query 810	AAAAAGGAGCAGCGAATGCAAAAGAAATCTGGGACAGAACCTAAAATGGCTCCTCAGGA	869		
Sbjct 305	AAAAAGGAGCAGCGAATGCAAAAGAAATCTGGGACAGAACCTAAAATGGCTCCTCAGGA	364		
Query 870	GAATCAGCTTCAAGAAAAGGAAAATCTAGGCCGTGATCTTCACTACCTGAGACGTCTAA	929		
Sbjct 365	GAATCAGCTTCAAGAAAAGGAAAATCTAGGCCGTGATCTTCACTACCTGAGACGTCTAA	424		
Query 930	AAAGGAGCACATCTCAGCTGAAAACATGTCTTTAGAACTCTGAGAAACAGCAGCCAGA	989		
Sbjct 425	AAAGGAGCACATCTCAGCTGAAAACATGTCTTTAGAACTCTGAGAAACAGCAGCCAGA	484		
Query 990	AGACCTCTTTGATGAGATT 1008			
Sbjct 485	AGACCTCTTTGATGAGATT 503			

V83_S105Del - REVERSE

Range 1: 6 to 400 [Graphics](#) ▼ Next Match ▲ Previous Match

Score	Expect	Identities	Gaps	Strand
719 bits(389)	0.0	394/396(99%)	1/396(0%)	Plus/Minus
Query 316	TTGAGACTTGGTTCCTTCAACCTAGAGAAAGTTGAAAACCCAGCTGAAGTCATTAGAGAA	375		
Sbjct 400	TTGAGACTTGGTTCCTTCAACCTAGAGAAAGTTGAAAACCCAGCTGAAGTCATTAGAGAA	341		
Query 376	CTTATTTGTTATTGCTTGGACACCATTCGAGAAAATCAAGCCAAAATGAGCACCTGCAG	435		
Sbjct 340	CTTATTTGTTATTGCTTGGACACCATTCGAGAAAATCAAGCCAAAATGAGCACCTGCAG	281		
Query 436	AAAGAAAATGAAAGCTTCTGAGAGATTGGAATGATGTTCAAGGACGATTTGAAAATGT	495		
Sbjct 280	AAAGAAAATGAAAGCTTCTGAGAGATTGGAATGATGTTCAAGGACGATTTGAAAATGT	221		
Query 496	GTGACTGCTAAGGAAGCTTTGGAGACTGATCTTTATAAGCGGTTTATTCTGGTGTGAAT	555		
Sbjct 220	GTGACTGCTAAGGAAGCTTTGGAGACTGATCTTTATAAGCGGTTTATTCTGGTGTGAAT	161		
Query 556	GAGAAGAAAACAAAATCAGAAAGTTGCAATAATAAATTTAAATGCAGCTCAAGAACGA	615		
Sbjct 160	GAGAAGAAAACAAAATCAGAAAGTTGCAATAATAAATTTAAATGCAGCTCAAGAACGA	101		
Query 616	GAAAAGGACATCAAAACAGAGGGGAACTGCAATCTGTTCTGAAATGACTGCTGACCGA	675		
Sbjct 100	GAAAAGGACATCAAAACAGAGGGGAACTGCAATCTGTTCTGAAATGACTGCTGACCGA	41		
Query 676	GATCCAGTCTATGATGAGAGTACTGATGAGGAAAGT 711			
Sbjct 40	GATCCAGTCTATGATGAGAGTACTGATGAG-AAAGT 6			

Range 2: 401 to 646 [Graphics](#) ▼ Next Match ▲ Previous Match ▲ First M

Score	Expect	Identities	Gaps	Strand
455 bits(246)	7e-132	246/246(100%)	0/246(0%)	Plus/Minus
Query 1	ATGGAGAGAAAATAAGCAGAAATCCACCTTGTTCCTGAACCCAGTATAACTCATTCTTA	60		
Sbjct 646	ATGGAGAGAAAATAAGCAGAAATCCACCTTGTTCCTGAACCCAGTATAACTCATTCTTA	587		
Query 61	CAAGTATCTTGGGAGAAAACACTGGAATCTGGTTTGTATTACACTTACTGATGGTCAT	120		
Sbjct 586	CAAGTATCTTGGGAGAAAACACTGGAATCTGGTTTGTATTACACTTACTGATGGTCAT	527		
Query 121	TCAGCATGGACTGGGACAGTTTCTGAATCAGAGATTTCCCAAGAACTGATGACATGGCA	180		
Sbjct 526	TCAGCATGGACTGGGACAGTTTCTGAATCAGAGATTTCCCAAGAACTGATGACATGGCA	467		
Query 181	ATGGAAAAGGGAAAATATGTTGGTGAACCTGAGAAAAGCATTTGTTCTCAGGAGCAGGACCA	240		
Sbjct 466	ATGGAAAAGGGAAAATATGTTGGTGAACCTGAGAAAAGCATTTGTTCTCAGGAGCAGGACCA	407		
Query 241	GCTGAT 246			
Sbjct 406	GCTGAT 401			

W43R - FORWARD

Range 1: 2 to 503 [Graphics](#) ▼ Next Match ▲ Previous Match

Score	Expect	Identities	Gaps	Strand
917 bits(496)	0.0	501/503(99%)	1/503(0%)	Plus/Plus
Query 506	AGGAAGCTTTGGAGACTGATCTTTATAAGCGGTTTATTCTGGTGTGAATGAGAAGAAAA			565
Sbjct 2	AGG-AGCTTTGGAGACTGATCTTTATAAGCGGTTTATTCTGGTGTGAATGAGAAGAAAA			60
Query 566	CAAAAATCAGAAGTTTGCATAATAAATATTAATAATGCAGCTCAAGAACGAGAAAAGGACA			625
Sbjct 61	CAAAAATCAGAAGTTTGCATAATAAATATTAATAATGCAGCTCAAGAACGAGAAAAGGACA			120
Query 626	TCAAACAAGAGGGGAAACTGCAATCTGTTCTGAAATGACTGCTGACCGAGATCCAGTCT			685
Sbjct 121	TCAAACAAGAGGGGAAACTGCAATCTGTTCTGAAATGACTGCTGACCGAGATCCAGTCT			180
Query 686	ATGATGAGAGTACTGATGAGGAAAGTGAACCAAACTGATCTCTCTGGGTTGGCTTCAG			745
Sbjct 181	ATGATGAGAGTACTGATGAGGAAAGTGAACCAAACTGATCTCTCTGGGTTGGCTTCAG			240
Query 746	CTGCTGAAGTAAAGATGATCCATTATTCAAGTCTTGATGTCACCTGATATTGCACCAA			805
Sbjct 241	CTGCTGAAGTAAAGATGATCCATTATTCAAGTCTTGATGTCACCTGATATTGCACCAA			300
Query 806	GTAGAAAAGGAGACAGCGAATGCAAAAGAAATCTTGGGACAGAACCTAAAAATGGCTCCTC			865
Sbjct 301	GTAGAAAAGGAGACAGCGAATGCAAAAGAAATCTTGGGACAGAACCTAAAAATGGCTCCTC			360
Query 866	AGGAGAATCAGCTTCAAGAAAAGGAAAATCTAGGCCTGATTCTTCACTACCTGAGACGT			925
Sbjct 361	AGGAGAATCAGCTTCAAGAAAAGGAAAATCTAGGCCTGATTCTTCACTACCTGAGACGT			420
Query 926	CTAAAAGGAGCACATCTCAGCTGAAAACATGCTTTAGAAACTCTGAGAAACAGCAGCC			985
Sbjct 421	CTAAAAGGAGCACATCTCAGCTGAAAACATGCTTTAGAAACTCTGAGAAACAGCAGCC			480
Query 986	CAGAAGACCTCTTTGATGAGATT	1008		
Sbjct 481	CAGAAGACCTCTTTGATGAGATT	503		

W43R - REVERSE

Range 1: 3 to 715 [Graphics](#) ▼ Next Match ▲ Previous Match

Score	Expect	Identities	Gaps	Strand
1301 bits(704)	0.0	711/714(99%)	1/714(0%)	Plus/Minus
Query 1	ATGGAGAGAAAAATAAGCAGAATCCACCTTGTTTCTGAACCCAGTATAACTCATTPTCTA			60
Sbjct 715	ATGGAGAGAAAAATAAGCAGAATCCACCTTGTTTCTGAACCCAGTATAACTCATTPTCTA			656
Query 61	CAAGTATCTTGGGAGAAAACACTGGAATCTGGTTTTGTTATTACACTTACTGATGGTCAT			120
Sbjct 655	CAAGTATCTTGGGAGAAAACACTGGAATCTGGTTTTGTTATTACACTTACTGATGGTCAT			596
Query 121	TCAGCATGGACTGGGACAGTTTCTGAATCAGAGATTTCCCAAGAAAGCTGATGACATGGGA			180
Sbjct 595	TCAGCATGGACTGGGACAGTTTCTGAATCAGAGATTTCCCAAGAAAGCTGATGACATGGGA			536
Query 181	ATGGAAAAGGGAAATATGTTGGTGAACCTGAGAAAAGCATTTGTTGTCAGGAGCAGGACCA			240
Sbjct 535	ATGGAAAAGGGAAATATGTTGGTGAACCTGAGAAAAGCATTTGTTGTCAGGAGCAGGACCA			476
Query 241	GCTGATGTATACACGTTTAAATTTTCTAAAAGAGTCTTGTATTCTTCTTTGAGAAAAAC			300
Sbjct 475	GCTGATGTATACACGTTTAAATTTTCTAAAAGAGTCTTGTATTCTTCTTTGAGAAAAAC			416
Query 301	CTGAAAGATGCTCATTACAGACTTGGTTCCTTCAACCTAGAGAAAGTTGAAAACCCAGCT			360
Sbjct 415	CTGAAAGATGCTCATTACAGACTTGGTTCCTTCAACCTAGAGAAAGTTGAAAACCCAGCT			356
Query 361	GAAGTCATTAGAGAACTTATTGTTATTGCTTGGACACCATTCAGAAAATCAAGCCAAA			420
Sbjct 355	GAAGTCATTAGAGAACTTATTGTTATTGCTTGGACACCATTCAGAAAATCAAGCCAAA			296
Query 421	AATGAGCACCTGCAGAAAAGAAAATGAAAGGCTTCTGAGAGATTGGAATGATGTTCAAGGA			480
Sbjct 295	AATGAGCACCTGCAGAAAAGAAAATGAAAGGCTTCTGAGAGATTGGAATGATGTTCAAGGA			236
Query 481	CGATTTGAAAAATGTTGAGTGCTAAGGAAGCTTTGGAGACTGATCTTTATAAGCGGTTT			540
Sbjct 235	CGATTTGAAAAATGTTGAGTGCTAAGGAAGCTTTGGAGACTGATCTTTATAAGCGGTTT			176
Query 541	ATTCTGGTGTGAATGAGAAGAAAACAAAAATCAGAAGTTTGCATAATAAATATTAATAAT			600
Sbjct 175	ATTCTGGTGTGAATGAGAAGAAAACAAAAATCAGAAGTTTGCATAATAAATATTAATAAT			116
Query 601	GCAGCTCAAGAACGAGAAAAGGACATCAAAACAGAGGGGAAAACGCAATCTGTTCTGAA			660
Sbjct 115	GCAGCTCAAGAACGAGAAAAGGACATCAAAACAGAGGGGAAAACGCAATCTGTTCTGAA			56
Query 661	ATGACTGCTGACCGAGATCCAGTCTATGATGAGAGTACTGATGAGGAAAGTGAA	714		
Sbjct 55	ATGACTGCTGACCGAGATCCAGTCTATGATGAGAGTACTGATGAG-AAAGTTAA	3		

D254Mfs*68 - FORWARD

Sequence ID: Query_152471 Length: 820 Number of Matches: 1

Range 1: 5 to 502		Graphics	Next Match	Previous Match
Score	Expect	Identities	Gaps	Strand
909 bits(492)	0.0	497/499(99%)	1/499(0%)	Plus/Plus
Query 510	AGCTTTGGAGACTGATCTTTATAAGCGGTTTATTCTGGTGTGAATGAGAAGAAAAA	569		
Sbjct 5	AGCTTTGGAGACTGATCTTTATAAGCGGTTTATTCTGGTGTGAATGAGAAGAAAAA	64		
Query 570	AATCAGAAGTTTGCATAATAAATTTAAATGCAGCTCAAGAACGAGAAAAGGACATCAA	629		
Sbjct 65	AATCAGAAGTTTGCATAATAAATTTAAATGCAGCTCAAGAACGAGAAAAGGACATCAA	124		
Query 630	ACAAGAAGGGGAACTGCAATCTGTTCTGAAATGACTGCTGACCGAGATCCAGTCTATGA	689		
Sbjct 125	ACAAGAAGGGGAACTGCAATCTGTTCTGAAATGACTGCTGACCGAGATCCAGTCTATGA	184		
Query 690	TGAGAGTACTGATGAGGAAAGTAAAACCAACTGATCTCTGGGTTGGCTCAGCTGC	749		
Sbjct 185	TGAGAGTACTGATGAGGAAAGTAAAACCAACTGATCTCTGGGTTGGCTCAGCTGC	244		
Query 750	TGTAAGTAAAGATGATCCATTATTTCAAGTCTTGATCTCACTGATATGCACCAAGTAG	809		
Sbjct 245	TGTAAGTAAAG-ATGATCCATTATTTCAAGTCTTGATCTCACTGATATGCACCAAGTAG	303		
Query 810	AAAAGGAGACGCGAATGCAAGAAATCTGGGACAGAACCTAAATGGCTCCTCAGGA	869		
Sbjct 304	AAAAGGAGACGCGAATGCAAGAAATCTGGGACAGAACCTAAATGGCTCCTCAGGA	363		
Query 870	GAATCAGCTTCAAGAAAAGGAAAATCTAGGCCTGATTTCACTACTGAGACGTCTAA	929		
Sbjct 364	GAATCAGCTTCAAGAAAAGGAAAATCTAGGCCTGATTTCACTACTGAGACGTCTAA	423		
Query 930	AAAGGACACATCTGAGTGAATCATGCTTTAGAACTCTGAGAAACGACGCCAGA	989		
Sbjct 424	AAAGGACACATCTGAGTGAATCATGCTTTAGAACTCTGAGAAACGACGCCAGA	483		
Query 990	AGACCTCTTGATGAGATT 1008			
Sbjct 484	AGACCTCTTGATGAGATT 502			

D254Mfs*68 - REVERSE

Sequence ID: Query_9783 Length: 820 Number of Matches: 1

Range 1: 3 to 715		Graphics	Next Match	Previous Match
Score	Expect	Identities	Gaps	Strand
1303 bits(705)	0.0	712/715(99%)	2/715(0%)	Plus/Minus
Query 1	ATGGAGAGAAAAAATAGCAGAATCCACCTTGTTTCTGAACCCAGTATAACTCATTTCCTA	60		
Sbjct 715	ATGGAGAGAAAAAATAGCAGAATCCACCTTGTTTCTGAACCCAGTATAACTCATTTCCTA	656		
Query 61	CAAGTATCTTGGGAGAAAACACTGGAACTCGGTTTGTATTACACTTACTGATGGTCAT	120		
Sbjct 655	CAAGTATCTTGGGAGAAAACACTGGAACTCGGTTTGTATTACACTTACTGATGGTCAT	596		
Query 121	TCAGCATGGACTGGGACAGTTTCTGAATCAGAGATTCCCAAGAAAGCTGATGACATGGCA	180		
Sbjct 595	TCAGCATGGACTGGGACAGTTTCTGAATCAGAGATTCCCAAGAAAGCTGATGACATGGCA	536		
Query 181	ATGAAAAAGGGAAATATGTTGGTGAACCTGAGAAAAGCATTGTTGTCAGGAGCAGGACCA	240		
Sbjct 535	ATGAAAAAGGGAAATATGTTGGTGAACCTGAGAAAAGCATTGTTGTCAGGAGCAGGACCA	476		
Query 241	GCTGATGTATACACGTTTAAATTTTCTAAAGAGTCTTGTTATTCTTCTTTGAGAAAAAC	300		
Sbjct 475	GCTGATGTATACACGTTTAAATTTTCTAAAGAGTCTTGTTATTCTTCTTTGAGAAAAAC	416		
Query 301	CTGAAAGATGTCTCATTGAGACTTGTTCTTCAACCTAGAGAAAGTTGAAAACCCAGCT	360		
Sbjct 415	CTGAAAGATGTCTCATTGAGACTTGTTCTTCAACCTAGAGAAAGTTGAAAACCCAGCT	356		
Query 361	GAAGTCATTAGAGAACTTATTTGTTATTGCTTGGACACCATGTCAGAAAAATCAAGCCAAA	420		
Sbjct 355	GAAGTCATTAGAGAACTTATTTGTTATTGCTTGGACACCATGTCAGAAAAATCAAGCCAAA	296		
Query 421	AATGAGCACCTGCAGAAAAGAAAATGAAAGGCTTCTGAGAGATTGGAATGATGTTCAAGGA	480		
Sbjct 295	AATGAGCACCTGCAGAAAAGAAAATGAAAGGCTTCTGAGAGATTGGAATGATGTTCAAGGA	236		
Query 481	CGATTTGAAAAATGTGTGAGTGTCTAAGGAAGCTTTGGAGACTGATCTTTATAAGCGGTTT	540		
Sbjct 235	CGATTTGAAAAATGTGTGAGTGTCTAAGGAAGCTTTGGAGACTGATCTTTATAAGCGGTTT	176		
Query 541	ATTCGGTGTGAATGAGAAGAAAACAAAATCAGAAGTTTGCATAATAAATATATAAAT	600		
Sbjct 175	ATTCGGTGTGAATGAGAAGAAAACAAAATCAGAAGTTTGCATAATAAATATATAAAT	116		
Query 601	GCAGCTCAGAACGAGAAAAGGACATCAAAACAGAGGGGAACTGCAATCTGTTCTGAA	660		
Sbjct 115	GCAGCTCAGAACGAGAAAAGGACATCAAAACAGAGGGGAACTGCAATCTGTTCTGAA	56		
Query 661	ATGACTGCTGACCGAGATCCAGTCTATGATGAGAGTACTGATGAG-AAAAGT-AAA	715		
Sbjct 55	ATGACTGCTGACCGAGATCCAGTCTATGATGAGAGTACTGATGAG-AAAAGT-AAA	3		

R161Q - Forward

pcMV10
150k25_R161Q_1_F (Arginine 65A to Glutamine 65A)

Sequence ID: ic1|Query_2453|Length: 820|Number of Matches: 1
Related Information
Range 1: 157 to 820|[Query](#)|[Subject](#)|[Next Match](#)|[Previous Match](#)

Alignment statistics for match #1

Score	Expect	Identities	Gaps	Strand
1216 bits (658)	0.0	643/665 (99%)	1/665 (0%)	Plus/Plus

Query 1 ATGAGAGAAAAAATAGCAGAAATCCAGCTTGTTCGAGCCGATATAGCTGATTTCTA 60
|||||
Sbjct 157 ATGAGAGAAAAAATAGCAGAAATCCAGCTTGTTCGAGCCGATATAGCTGATTTCTA 216

Query 61 CAAGTATCTTGGGAGAAACCTGGAATCTGTTTGTATTACACTACTGATGTTGTCAT 120
|||||
Sbjct 217 CAAGTATCTTGGGAGAAACCTGGAATCTGTTTGTATTACACTACTGATGTTGTCAT 276

Query 121 TCAGATGCACTGGACAGTTTCTGATCGAGATTTCCAGAAAGCTGATCGACTGGCA 180
|||||
Sbjct 277 TCAGATGCACTGGACAGTTTCTGATCGAGATTTCCAGAAAGCTGATCGACTGGCA 336

Query 181 ATGCAAAAAGGGAATATGTTGCTGCACTGAGAAAGCATGTTGTCAGCAGCAGACCA 240
|||||
Sbjct 337 ATGCAAAAAGGGAATATGTTGCTGCACTGAGAAAGCATGTTGTCAGCAGCAGACCA 396

Query 241 GCTGATGATACAGTTAATTTTCTAAGAGCTGTTGATTTCTCTTTGAGAAAAAC 300
|||||
Sbjct 397 GCTGATGATACAGTTAATTTTCTAAGAGCTGTTGATTTCTCTTTGAGAAAAAC 456

Query 301 CTGAAGATGCTGATTCAGACTGTTTCTTCAAGCTAGAGAAAGTGGAAAAACAGCT 360
|||||
Sbjct 457 CTGAAGATGCTGATTCAGACTGTTTCTTCAAGCTAGAGAAAGTGGAAAAACAGCT 516

Query 361 GAAGTATAGAGAACTATTGTTATGCTTGCAGCAGCATTCGAGAAAAATCAAGGAAA 420
|||||
Sbjct 517 GAAGTATAGAGAACTATTGTTATGCTTGCAGCAGCATTCGAGAAAAATCAAGGAAA 576

Query 421 AATGAGCAGCTGAGAAAAAATGAAAGGCTTCTGAGAGATTGAAATGATGTTCAAGGA 480
|||||
Sbjct 577 AATGAGCAGCTGAGAAAAAATGAAAGGCTTCTGAGAGATTGAAATGATGTTCAAGGA 636

Query 481 CAAATTTGAAAAATGTTGAGTGTAGGAAGGCTTTGGACAGTATCTTTAAGAGGTTT 540
|||||
Sbjct 637 CAAATTTGAAAAATGTTGAGTGTAGGAAGGCTTTGGACAGTATCTTTAAGAGGTTT 696

Query 541 ATTCTGGTCTGAAATGAGAGAAACAAAATCGAGAGTTTCATATAAATATTAAT 600
|||||
Sbjct 697 ATTCTGGTCTGAAATGAGAGAAACAAAATCGAGAGTTTCATATAAATATTAAT 756

Query 601 GCAGCTCAAGAGCAGAAAGAGCAGATCAAGAGAAAGGAGAACTGCAATCTGTTCTGAA 660
|||||
Sbjct 757 GCAGCTCAAGAGCAGAAAGAGCAGATCAAGAGAAAGGAGAACTGCAATCTGTTCTGAA 815

Query 661 ATGAC 665
|||||
Sbjct 816 ATGAC 820

OK!

R161Q - Reverse

pcMV10
150k25_R161Q_1_R (Arginine 65A to Glutamine 65A)

Sequence ID: ic1|Query_4563|Length: 820|Number of Matches: 1
Related Information
Range 1: 101 to 820|[Query](#)|[Subject](#)|[Next Match](#)|[Previous Match](#)

Alignment statistics for match #1

Score	Expect	Identities	Gaps	Strand
1314 bits (711)	0.0	717/728 (99%)	8/728 (1%)	Plus/Minus

Query 209 TTTGAGAAAAATCGAAGATGCTGATTCAGACTGGTTCCTCAAGCTAGAGAAAGTT 348
|||||
Sbjct 820 TTTGAGAAAAATCGAAGATGCTGATTCAGACTGGTTCCTCAAGCTAGAGAAAGTT 761

Query 348 GAAMACAGCTGACAGTATAGAGAACTATTGTTATGCTTGGACAGCATTCAGAAA 408
|||||
Sbjct 760 GAAMACAGCTGACAGTATAGAGAACTATTGTTATGCTTGGACAGCATTCAGAAA 701

Query 407 AATGAGCCAAAATGAGAGCTTCGAAAGAAAATGAAAGGCTTCGAGAGATTGGAA 468
|||||
Sbjct 700 AATGAGCCAAAATGAGAGCTTCGAAAGAAAATGAAAGGCTTCGAGAGATTGGAA 641

Query 469 GAGTTGAGAGAAATTTGAAAAATGTTGAGTGTGAGAGAGGCTTTGAGAGCTGATCT 528
|||||
Sbjct 640 GAGTTGAGAGAAATTTGAAAAATGTTGAGTGTGAGAGAGGCTTTGAGAGCTGATCT 581

Query 529 TAFAGGAGTATTTGAGGCTTGAATGAGAGAAACAAAATCGAGAGTTTGATAAT 588
|||||
Sbjct 580 TAFAGGAGTATTTGAGGCTTGAATGAGAGAAACAAAATCGAGAGTTTGATAAT 521

Query 589 AAATTAATGAGCTCAAGAGCAGAAAGGACATCAAGCAAGGCGCAACTGCA 648
|||||
Sbjct 520 AAATTAATGAGCTCAAGAGCAGAAAGGACATCAAGCAAGGCGCAACTGCA 661

Query 649 ATGTTGTGAAATGAGCTTCGAGAGAAATGAGAGTTCGATGAGAGCTGATGAGAA 708
|||||
Sbjct 460 ATGTTGTGAAATGAGCTTCGAGAGAAATGAGAGTTCGATGAGAGCTGATGAGAA 601

Query 709 AATGAAAGCAACTGATCTCTGAGGCTTGGCTTCAGCTGCTGATAGTAAAGATGATTC 768
|||||
Sbjct 400 AATGAAAGCAACTGATCTCTGAGGCTTGGCTTCAGCTGCTGATAGTAAAGATGATTC 341

Query 769 ATATTTCAGCTCTGATCTCTGATGATATTCAGCACTAGAAAGAGAGAGAGAGATC 828
|||||
Sbjct 340 ATATTTCAGCTCTGATCTCTGATGATATTCAGCACTAGAAAGAGAGAGAGAGATC 281

Query 829 CAAGAAATCTGGAGAGAGCTTAAATGGCTCTGAGAGAAATCAGCTTCAAGAAAG 888
|||||
Sbjct 280 CAAGAAATCTGGAGAGAGCTTAAATGGCTCTGAGAGAAATCAGCTTCAAGAAAG 221

Query 889 GAAMATCTAGGCTGATCTTCACTACTGAGAGCTTAAAGAGAGAGAGATCTGAGCT 948
|||||
Sbjct 220 GAAMATCTAGGCTGATCTTCACTACTGAGAGCTTAAAGAGAGAGAGATCTGAGCT 161

Query 949 CAAGAGCTCTTTAGAACTCTGAGAGAGAGAGAGAGAGAGAGAGAGAGAGAGAGAT 1008
|||||
Sbjct 160 CAAGAGCTCTTTAGAACTCTGAGAGAGAGAGAGAGAGAGAGAGAGAGAGAGAT 901

OK!

Appendix 3 - Sequence Check After Mutagenesis of XRCC4 Mutation Associated to Cancer Risk

A247S - FORWARD

Range 1: 4 to 502		Graphics			▼ Next Match ▲ Previous Match
Score	Expect	Identities	Gaps	Strand	
911 bits(493)	0.0	497/499(99%)	0/499(0%)	Plus/Plus	
Query 510	AGCTTTGGAGACTGATCTTTATAAGCGGTTTATTTCTGGTGTGAATGAGAAGAAAAACAAA	569			
Sbjct 4	AGCTTTGGAGACTGATCTTTATAAGCGGTTTATTTCTGGTGTGAATGAGAAGAAAAACAAA	63			
Query 570	AATCAGAAGTTTGCATAATAAATTTAATAATGCAGCTCAAGAACGAGAAAAAGGACATCAA	629			
Sbjct 64	AATCAGAAGTTTGCATAATAAATTTAATAATGCAGCTCAAGAACGAGAAAAAGGACATCAA	123			
Query 630	ACAAGAAGGGGAAACTGCAATCTGTTCTGAAATGACTGCTGACCGAGATCCAGTCTATGA	689			
Sbjct 124	ACAAGAAGGGGAAACTGCAATCTGTTCTGAAATGACTGCTGACCGAGATCCAGTCTATGA	183			
Query 690	TGAGAGTACTGATGAGGAAAGTGA AACCAA ACTGATCTCTCGGGTTGGCTTCAGCTGC	749			
Sbjct 184	TGAGAGTACTGATGAGGAAAGTGA AACCAA ACTGATCTCTCGGGTTGGCTTCAGCTGC	243			
Query 750	TGTAAGTAAAGATGATTCATTATTTCAAGTCTTGATGCTCACTGATATTGCACCAAGTAG	809			
Sbjct 244	TGTAAGTAAAGATGATTCATTATTTCAAGTCTTGATGCTCACTGATATTGCACCAAGTAG	303			
Query 810	AAAAAGGAGACAGCGAATGCAAGAAATCTGGGACAGAACCTAAAATGGCTCCTCAGGA	869			
Sbjct 304	AAAAAGGAGACAGCGAATGCAAGAAATCTGGGACAGAACCTAAAATGGCTCCTCAGGA	363			
Query 870	GAATCAGCTTCAAGAAAAGGAAAAATTTAGGCCCTGATTTCTTCACTACCTGAGACGTCTAA	929			
Sbjct 364	GAATCAGCTTCAAGAAAAGGAAAAATTTAGGCCCTGATTTCTTCACTACCTGAGACGTCTAA	423			
Query 930	AAAGGAGCACATCTCAGCTGAAAACATGCTTTAGAACTCTGAGAAACAGCAGCCGAGA	989			
Sbjct 424	AAAGGAGCACATCTCAGCTGAAAACATGCTTTAGAACTCTGAGAAACAGCAGCCGAGA	483			
Query 990	AGACCTCTTTGATGAGATT	1008			
Sbjct 484	AGACCTCTTTGATGAGATT	502			

A247S – REVERSE

Range 1: 5 to 714		Graphics			▼ Next Match ▲ Previous Match
Score	Expect	Identities	Gaps	Strand	
1301 bits(704)	0.0	709/711(99%)	1/711(0%)	Plus/Minus	
Query 1	ATGGAGAGAAAAATAAGCAGAATCCACCTTGTCTTGAACCCAGTATAAATCAATTTTCTA	60			
Sbjct 714	ATGGAGAGAAAAATAAGCAGAATCCACCTTGTCTTGAACCCAGTATAAATCAATTTTCTA	655			
Query 61	CAAGTATCTTGGGAGAAAACACTGGAATCTGGTTTGTATTACACTTACTGATGGTCAT	120			
Sbjct 654	CAAGTATCTTGGGAGAAAACACTGGAATCTGGTTTGTATTACACTTACTGATGGTCAT	595			
Query 121	TCAGCATGGACTGGGACAGTTTCTGAATCAGAGATTTCCCAAGAAGCTGATGACATGGCA	180			
Sbjct 594	TCAGCATGGACTGGGACAGTTTCTGAATCAGAGATTTCCCAAGAAGCTGATGACATGGCA	535			
Query 181	ATGGA AAAAGGAAAATATGTTGGTGAAC TGAGAAAAGCATTGTTGTCAGGAGCAGGACCA	240			
Sbjct 534	ATGGA AAAAGGAAAATATGTTGGTGAAC TGAGAAAAGCATTGTTGTCAGGAGCAGGACCA	475			
Query 241	GCTGATGTATACACGTTTAAATTTTCTAAAGAGTCTTGTATTTCCTCTTGAGAAAAAC	300			
Sbjct 474	GCTGATGTATACACGTTTAAATTTTCTAAAGAGTCTTGTATTTCCTCTTGAGAAAAAC	415			
Query 301	CTGAAAGATGCTCATTTCAGACTTGGTTCCTCAACCTAGAGAAAGTTGAAAACCCAGCT	360			
Sbjct 414	CTGAAAGATGCTCATTTCAGACTTGGTTCCTCAACCTAGAGAAAGTTGAAAACCCAGCT	355			
Query 361	GAAGTCATTAGAGAACTTATTTGTTATTGCTTGGACACCATTCAGAAAAACAAGCCAAA	420			
Sbjct 354	GAAGTCATTAGAGAACTTATTTGTTATTGCTTGGACACCATTCAGAAAAACAAGCCAAA	295			
Query 421	AATGAGCACCTGCAGAAAAGAAAATGAAAGGCTTCTGAGAGATTGGAATGATGTTCAAGGA	480			
Sbjct 294	AATGAGCACCTGCAGAAAAGAAAATGAAAGGCTTCTGAGAGATTGGAATGATGTTCAAGGA	235			
Query 481	CGATTTGAAAAATGTGTAGTGTAAAGGAACTTTGGAGACTGATCTTTATAAGCGGTTT	540			
Sbjct 234	CGATTTGAAAAATGTGTAGTGTAAAGGAACTTTGGAGACTGATCTTTATAAGCGGTTT	175			
Query 541	ATTCGGTGTGAATGAGAAGAAAACAAAATCAGAAGTTTGCATAATAAATTTATAAAT	600			
Sbjct 174	ATTCGGTGTGAATGAGAAGAAAACAAAATCAGAAGTTTGCATAATAAATTTATAAAT	115			
Query 601	CGAGCTCAAGAACGAGAAAAGGACATCAAAACAGAGGGGAACTGCAATCTGTTCTGAA	660			
Sbjct 114	CGAGCTCAAGAACGAGAAAAGGACATCAAAACAGAGGGGAACTGCAATCTGTTCTGAA	55			
Query 661	ATGACTGCTGACCGAGATCCAGTCTATGATGAGAGTACTGATGAGGAAAGT	711			
Sbjct 54	ATGACTGCTGACCGAGATCCAGTCTATGATGAGAGTACTGATGAG-AAAAGT	5			